Effect of Junction Aggregation on the Dynamics of Supramolecular Polymers and Networks

Mostafa Ahmadi, Amir Jangizehi,* Kay Saalwächter, and Sebastian Seiffert*

Transient structures based on associative polymers can deliver complex functions; as such, they hold promise for advanced applications as in drug delivery, tissue engineering, and electronics. The network structure and timescale of its rearrangement are key factors that define their range of utility. However, the inevitable phase separation of polar pairwise associations from nonpolar polymer chains frequently causes junction aggregation, whose stability and functionality significantly affect the network structure and dynamics, and as such, redefine its utility. Engineering the extent of association is a necessity for controlling properties of supramolecular materials, yet the current knowledge of the effect of design parameters on specificities of aggregates and their consequent effects on material properties is limited. To address this gap, the importance of aggregation is highlighted, the available theories and models of the dynamics of associative polymers in the presence of aggregates are reviewed, and the existing experimental records to draw a general guideline for interpreting the effect of aggregates on polymer dynamics are classified. Moreover, pitfalls and considerations like the applicability of time–temperature superposition, and the interplay of kinetics and thermodynamics of aggregation that may undermine the authenticity of the reported data are reviewed.

1. Introduction

Supramolecular chemistry can be defined as the science of integration of physical/transient bonds to design functional materials.[1,2] The outcome is different classes of materials, in which physical bonds result in specific transient architectures,

M. Ahmadi, A. Jangizehi, S. Seiffert
Department of Chemistry
Johannes Gutenberg University Mainz
Duesbergweg 10–14, 55128 Mainz, Germany
E-mail: amir.jangizehi@uni-mainz.de; sebastian.seiffert@uni-mainz.de

K. Saalwächter
Institut für Physik – NMR
Martin-Luther-Universität Halle-Wittenberg
Betty-Heimann-Str. 7, 06120 Halle (Saale), Germany

dynamics, mechanical properties, or functions. The arrangement of small-molecule supramolecular units, i.e., molecules that carry associative groups with the possibility of forming physical bonds by transient association, leads to a range of molecular structures and mesoscopic morphologies arcing from linear/branch polymer architectures and percolated networks to micelles, columns, nanowires, and nanotubes, that form upon secondary interactions among pairwise associations.[3–5] Nevertheless, the design of supramolecular materials can be initiated from macromolecular units, where associative groups, frequently called stickers in this context, are emplaced at chain ends, as in telechelic associative polymers, or regularly/non-regularly grafted along the polymer backbone, as in side-chain systems. As such, transient pairwise association of stickers results in chain extension or network formation, respectively, which upon secondary interaction may even lead to ordered transient structures and morphologies similar to those that could be obtained from the small-molecule counterparts.

One of the main features of physical bonds is their dynamic nature, with a practically accessible bond lifetime under ambient conditions. As such, by applying appropriate stimuli, these bonds are reversibly broken/dissociated, which can reform/reassociate if those stimuli are removed and the required activation energy is provided. As a result, supramolecular materials are stimuli-responsive, with a high potential to be served as functional materials in advanced applications. One of the main elements of the design of such materials is controlling their dynamics, which in turn defines the rate of their stimuli-responsiveness and the lifetime of their functions. The dynamics of supramolecular polymer materials depend not only on the dynamics of transient bonds but also on dynamics of polymer backbones that carry supramolecular groups.[6,7]

On top of that, aggregation of transient bonds and stickers caused by the incompatibility of stickers with the surrounding medium and/or by the creation of secondary interactions between stickers has a significant influence on the dynamics of supramolecular materials. We have recently reviewed the origin and different pathways for aggregation of supramolecular units in polymeric systems, elsewhere.[8] Briefly, supramolecular units commonly phase separate into irregular domains due to

**ADVANCED
SCIENCE NEWS**

www.advancedsciencenews.com

[M] acro-molecular
Chemistry and Physics

www.mcp-journal.de

the common difference in thermodynamics specificities of stickers and the surrounding (macro)molecules. The aggregation phenomenon and domains formed by this process are known also as collective assembly and clusters, respectively. The irregular aggregates inside clusters can subsequently rearrange and create hierarchical assemblies through secondary interactions and form clusters of ordered structures. Alternatively, specifically in small-molecule supramolecular units, the initial binding may facilitate the secondary interaction, and therefore, result in a nucleation-growth mechanism, and bypass the formation of irregular aggregates.[8,9]

Aggregation is crucial for the structural stability and functions of numerous biomaterials in nature. The double helix structure of DNA is a result of hydrogen bonding between nucleobases (cytosine, guanine, adenine, uracil) of nucleotides, which are stabilized by base-stacking interactions between aromatic nucleobases.[10–12] Similarly, the amyloid fibrils are aggregations of folded cellular proteins into large and ordered, fibrillar proteins with predominantly β-sheet secondary structures.[13] The intermolecular binding within amyloid fibrils involves several different interactions, including $\pi-\pi$ stacking and hydrogen bonding.[14] Amyloid fibril formation is a common characteristic of different diseases like diabetes II. However, it can fulfill useful functions in various biological systems.[15] In the same way, there are countless examples in artificial, synthetic supramolecular materials, in which sticker clustering is elemental in formation, structural stability, properties, or functions. One of the key features that connect all of these apparently different aspects is the effect of clustering on dynamic properties.[16,17]

In this review, we focus on dynamics of supramolecular materials in the presence of junction aggregates. The main body of this paper focuses on synthetic supramolecular polymers and networks. To highlight the significance of this topic, in Section 2, we first highlight the importance of aggregation in supramolecular polymers at three different levels. In Section 3 the most important theories and models that have been developed for explaining the dynamics of associative polymers in the presence of clusters and dynamics of clusters are discussed. Finally, in Section 4, the most important experimental records that help understand practical aspects of chain dynamics in the presence of aggregates are discussed.

2. Importance of Aggregation

The importance of the aggregation of stickers in supramolecular materials can be viewed on three levels. On the first level, functions of supramolecular materials are derived from the existing transient bonds and do not depend on their aggregation. In this case, the importance of sticker clustering is limited to their influence on mechanical properties like the usual enhancement of (elastic) modulus. This enhancement partially compensates for the weak mechanical strength of supramolecular materials compared to equivalent materials that almost have the same microstructure but with covalent bonds. Self-healing supramolecular materials are probably one of the best examples that can be sorted at this level. In principle, the ability of self-healing is the result of the transient nature and stimuli-responsiveness of supramolecular bonds independent of sticker clustering. However, due to the inherent compromise

between mechanical robustness and self-healing ability, the phase separation of stickers and their aggregation can be considered in the design of self-healing supramolecular materials to preserve the required mechanical performance.[18,19] To force strong clustering, Guan and coworkers developed a multi-phase platform.[20–22] In this approach, the molecular platform consists of at least two incompatible units, where one type carries transient bonds. Due to the thermodynamic incompatibility between these units, strong phase separation occurs and commonly leads to the formation of nanodomains. For instance, a hybrid brush consisting of a polystyrene (PS) backbone with polyacrylate branches, where each repeating unit of branch chains ended with an imidazole group created a core-shell nanostructure,[20] the core consisting of the hard PS and the shell containing soft polyacrylate chain, as illustrated in **Figure 1**a. The combination of the core–shell nanostructure and the self-assembly between branch chains through the coordination with Zn^{2+} metal ions make a two-phase nanostructure, which shows stress–strain behavior like thermoplastic elastomers. The mechanical properties are adjusted by varying PS content, which can reach the elastic modulus of up to 36 MPa. In parallel, it shows a self-healing efficiency of up to 90% at ambient temperature without the need for any external stimulus. This ability comes from the self-assembly of branch chains by weak coordinative bonds between imidazole end groups and metal ions. A similar phase-separated network of hard PS/soft polyacrylate branch copolymer, where repeating units of branches are ended with an amide group shows a comparable combination of mechanical robustness and self-healing ability at ambient conditions due to the formation of dynamic hydrogen bonds between amide groups.[20]

On the next level, functions of supramolecular materials only emerge upon the phase separation of stickers and their aggregation. This notion of aggregation-induced function is employed in the development of all-season viscosity thickeners for engine oils based on telechelic and block copolymers. Triblock polymer chains, which contain a long soluble central segment and two short insoluble external ones, can associate and form micellar aggregates with a larger association tendency at higher temperatures. As such, the formation of a transient network of bridged micellar aggregates can significantly raise the viscosity.[23] In this category, materials that obtain their mechanical function from the aggregation of associative bonds can be also included. The pairwise heterocomplementary association of telechelic, low-T_g linear hydrophobic oligomers, which are end-functionalized with weak hydrogen bonding groups like adenine, cytosine, guanine, thymine, or uracil derivatives should only result in chain extension. However, some of these materials have demonstrated network-like properties such as the appearance of distinct elastic modulus, which is extended over a wide range of frequencies or temperatures, upon homocomplementary association. This cannot be explained unless considering a phase-separated network junction. Rowan and coworkers showed that the self-assembly of low-molar mass poly(tetrahydrofuran) (PTHF), terminated with adenine and cytosine derivatives yields materials with film and fiber forming capability, as illustrated in Figure 1b.[24] Such network-like properties are also observed upon sticker clustering of telechelic polymers end-functionalized with nucleobase derivatives.[25–28]
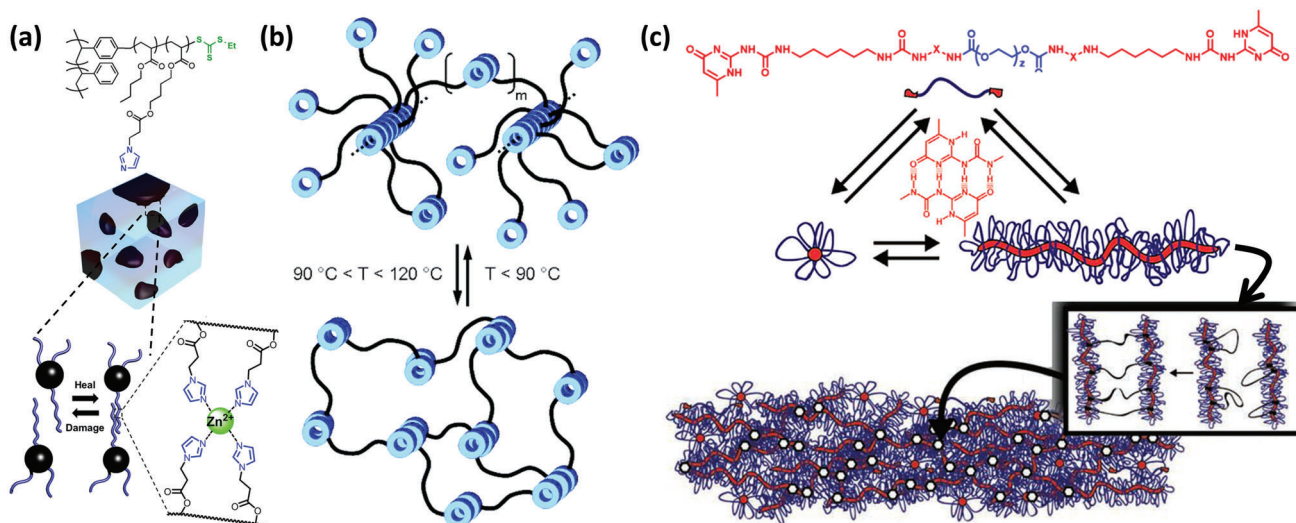
**ADVANCED
SCIENCE NEWS**

www.advancedsciencenews.com

Macro-
molecular
Chemistry and Physics

www.mcp-journal.de

Figure 1. Examples of the aggregation significance: a) Supplementing material properties in multi-phase self-healing materials. Adapted with permission.[22] Copyright 2014, American Chemical Society. b) Aggregation-induced properties in film and fiber forming telechelic associative polymers. Adapted with permission.[24] Copyright 2005, American Chemical Society. c) Aggregation-induced structure and properties in hydrogels based on hydrogen-bonded telechelic precursors. Adapted with permission.[35] Copyright 2012, Wiley.

On the third level, beyond functions and properties, the formation of supramolecular materials itself depends on the clustering of supramolecular units. In this case, without the clustering phenomenon, the pairwise association of stickers is not strong enough to stabilize any structure. The self-assembly of π-conjugated molecules by stacking aromatic units in one direction, which can be promoted with secondary hydrogen bonding, can potentially form structures with electronic functions like charge or energy transfer.[29] This approach can be employed in the self-assembly of small-molecule, oligomeric and polymeric units, where in most cases the combination of secondary interactions with the primarily π-conjugation is necessary to obtain ordered nano-objects.[30] In general, the structure of the π-stacking building block, its substitutions on the aromatic ring, and the type, number, and strength of secondary interactions have direct influences on the self-assembled nanostructure, and therefore, on their consequent properties. For example, in oligo(p-phenylene vinylene) derivatives with diamino triazine hydrogen-bonding associative group, the combination of π-conjugation of p-phenylenevinylene backbone and hydrogen bonding of diamino triazine leads to a hexameric π-conjugated rosette that self-assembles into chiral tubular objects following a two-step process including a transition from molecularly dissolved species into achiral stacks and then further development of helical bundles.[31] Mixed supramolecular stacks of such oligomers, e.g., mixing mono- and bi-functional precursors show ultrafast energy transfer from the short assemblies to long ones.[32] This concept has been used in light-emitting color tuning to show that recognition sites are electro- and photochemically inert.[30] Such an oligomeric backbone can also provide gels with helical morphologies if decorated with chiral chains.[33] This structure has potential applications for light harvesting and energy transfer to an incorporated dye.[34] Another example is the development of supramolecular assemblies based on shielding hydrogen bonds in water, which otherwise weaken or dissociate in aqueous media. This can be achieved, for example, by using a segmental hydrophilic-hydrophobic molecular platform, in which phase separation of these segments protects stickers from competitive interaction with water. With this concept, supramolecular hydrogels based on ureidopyrimidinone (UPy) groups are prepared. The molecular scaffold is poly(ethylene glycol) (PEG) end-functionalized with UPy groups, where short alkyl spacers (C_8-C_{12}) between UPy groups and PEG backbone shield hydrogen bonds.[35] In addition, the lateral hydrogen bonding between urea groups, which are used to link UPy groups and alkyl chains has a key role in stacking and stabilizing hydrogen-bonded UPy dimers, as shown in Figure 1c. The onset concentration of gel formation depends strongly on the length of the alkyl spacer and that of the polymer backbone. These materials form a combination of small micellar assemblies and high aspect ratio nanofibers in water and long fibrous structures in the neat bulk phase. Indeed, the shielding of hydrogen-bonded UPy dimers by hydrophobic pocket provided by the alkyl spacers was found responsible for the stability of the structure in water. The fibrillar structure is also the result of the lateral hydrogen bonds provided by urea linkages, where the inter-nanofiber connection by entanglement, aggregation, and/or supramolecular crosslinking is necessary to create a percolated network. Drugs and biological cargo are loaded in these hydrogels and transferred by minimally invasive injection thanks to their thixotropic behavior. In addition, the gelation depends on the pH of the environment, with no gelation happening at pH > 8.5.[36–38] This feature allows a great potential to use them as injectable hydrogels starting from a solution at high pH followed by post-injection gelation at physiological conditions.

As useful and sometimes essential as the introduction of aggregation in polymeric systems seems to be, the control of aggregation characteristics is challenging. The morphology and extent of aggregation depend on many variables like the chain length and chemical composition of precursors, the thermodynamic

**ADVANCED
SCIENCE NEWS**

www.advancedsciencenews.com

$\left[\substack{M}\right]$ acro-
molecular
Chemistry and Physics

www.mcp-journal.de

difference between the polarity of the polymer backbone and the pairwise associations, and on top of them, specifically in entangled polymeric systems, it is a compromise between kinetics and thermodynamics. Therefore, it is necessary to first realize how binary associations and their aggregation affect the structure and dynamics of networks, and how these effects can be explained in terms of models, as respectively detailed in Section 3.

3. Theory

The quantitative description of the complex relaxation process of long entangled polymer chains has been significantly simplified by the development of mean-field theories, which consider a universal relaxation process for chains with a specific topology and length. In this picture, chains in the bulk relax the same way as the probe chain does; therefore, one can replace neighboring chains with a mean-field environment.[39] This environment is treated just as average monomeric friction in the Rouse model, which is valid for long chains in dilute solutions, short unentangled chains in bulk, and on length scales shorter than the spacing between two subsequent entanglements in well-entangled systems. In tube-based relaxation mechanisms of well-entangled chains like reptation and contour length fluctuations (CLF) the environment, which is defined by the entanglement with neighboring chains, forms a hypothetical tube that limits the lateral movement but determines a curvilinear diffusion path for the probe chain.[40,41] As chains in the environment also move, this tube can reform and move laterally, which is captured by the so-called constraint release (CR) mechanism. At the same time, the removal of the entanglement constraints by the diffusion of neighboring chains leads to an increase in the effective tube diameter by the so-called dynamic tube dilation (DTD) mechanism, which accelerates the relaxation of the probe chain by reptation and CLF.[42] Details of these mechanisms and their extension to the case where binary associations and aggregation exist will be represented in Sections 3.3 and 3.4. But before that one needs to discuss the concentration/functionalization regimes where the mean-field approach may not be valid.

3.1. Dynamics of Associative Polymers

The general approach for describing the complex relaxation process of sticky chains, i.e., chains that are functionalized with groups that form transient bonds with a specific lifetime, follows the same mean-field approach. In this picture, chains with a specific topology and length can relax in the same way. However, chains with terminal sticky groups, i.e., telechelic chains, relax differently from those with stickers along the backbone, i.e., side-chain systems. The sticky Rouse and sticky reptation mechanisms, by Leibler, Semenov, Rubinstein, and Colby are classical pictures for describing the relaxation of unentangled and entangled side-chain systems.[43–46] Simply said, they are extensions of classical Rouse and reptation mechanisms in the presence of equidistant stickers with specific lifetimes along the backbone. Similarly, the relaxation of transient chains formed by the pairwise association of telechelic precursors is described by the reptation of living chains as suggested by Cates.[47] However, besides

topology and length, concentration and the number of stickers per chain can define different regimes of relaxation.[48–50]

Amin and coworkers have shown that for strongly associative groups, i.e., with high association energies above $10k_BT$, almost all stickers are effectively bound at every instant in time.[51] As such, long side-chain associative polymers with more than two junctions per chain can form an effectively percolated network, where the mean-field approach is valid. However, there is a critical number of stickers per chain, below which the percolation is lost and a fraction of chains can be regarded as an isolated cluster of soluble associated chains.[50] The relaxation of such chains can follow the polymeric dynamics and differ from the chains in the percolated network.[44,45] Of course, this critical number of stickers per chain depends on, and decreases with, the association strength. Therefore, the association strength and the degree of functionalization are independent but interchangeable parameters, i.e., it is possible to have the same regime of relaxation by keeping one constant and changing the other.[50]

For the equivalent classical condensation homopolymerization of the A_f monomer, where f represents the monomer functionality, the critical gel point is given by $p_c = 1/(f − 1)$. An analogous gel point can be defined for strongly associative chains, with infinite association strength, as $p_c = 1/(N − 1)$, where N is the degree of polymerization and p_c is the critical fraction of stickers beyond which network percolation happens. This corresponds to one crosslink, or equally two stickers, per chain. Chen and coworkers have defined a relative degree of functionalization, as $\epsilon = (p − p_c)/p_c$, and used it instead of concentration to determine different regimes of gelation, as illustrated in **Figure 2**.[48,50,52–54] Accordingly, the mean-field treatment of sticky chains is not expected to be valid around the gel point, i.e., at -1 < ϵ < 1. The isolated soluble chains have a distribution in size and topology, which results in a broad polymeric relaxation while the dynamics of other chains associated with a percolated network are governed by a defined kinetics of transient association. The mean-field approach also lacks to include the local heterogeneities in the percolated network namely, higher-order connectivities, loops, and dangling ends.[55] With that consideration, the mean-field approach is only valid for fully percolated networks at $\epsilon \geq 1$.

Accordingly, Rubinstein and Semenov have developed scaling laws for the linear viscoelastic properties of unentangled and entangled associative polymers in different regimes of gelation.[44–46] The most important parameters are the chain relaxation time, the elastic modulus, and consequently the zero-shear viscosity, which are connected as $\eta \sim \tau G$. For unentangled precursors, the lifetimes of transient associations are likely to be larger than the Rouse relaxation time. Therefore, transient association results in the formation of transient structures, which are isolated below the gel point and start to percolate beyond it. Below the gel point, i.e., $\epsilon < 0$, the system is composed of isolated soluble chain clusters with sparse associations, the number, and dispersity of which increases with ϵ, as shown in Figure 2. Longer transient chains may even get entangled; therefore, they relax much slower than shorter unentangled transient chains. Nevertheless, all chains relax by chain mechanisms like Rouse and reptation as the lifetime of associations is larger than chain dynamics. However, there is a critical degree of functionalization, $− \epsilon_c$, beyond which dissociation of transient bonds becomes faster than the final relaxation of long transient
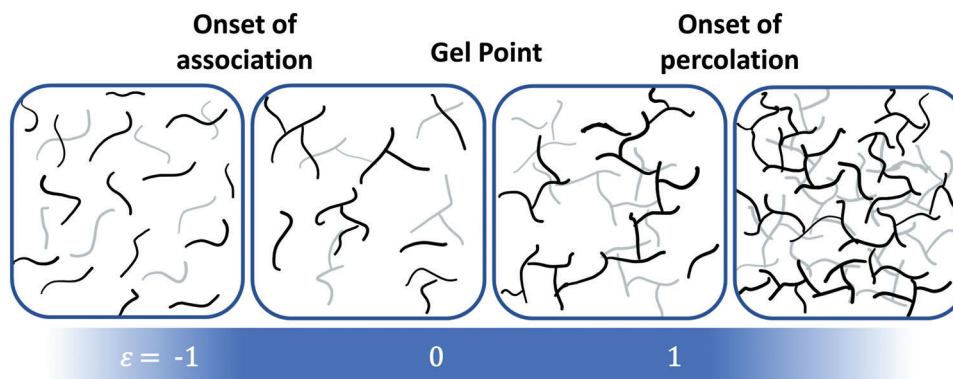
Figure 2. Variation of the structure composition in associative polymers by increasing the concentration or equivalently the relative degree of functionalization, ϵ; arcing from isolated chains to soluble transient extended chains, to the copresence of partially percolated networks and soluble clusters of extended chains, and to a fully percolated network.

clusters. Therefore, at $\epsilon < -\epsilon_c$ isolated clusters relax before the breakup, similar to gelation with permanent crosslinks, but above that, i.e., at $\epsilon > -\epsilon_c$, they break into smaller clusters before relaxing by chain dynamics.

Above the gel point, i.e., $0 < \epsilon < 1$, the system is composed of a percolated network as well as isolated soluble clusters of associated chains. The relaxation of the soluble part follows chain dynamics depending on their length, but the network chains should wait for the effective breakup to relax. Dissociated stickers may come back to their previous partners several times before finding a new free sticker; nevertheless, dissociation contributes to stress relaxation only if it ends in an effective partner exchange. In analogy to the previous regime, there is also a critical degree of functionalization, ϵ_c, beyond which the final relaxation of subclusters, formed after a single dissociation step, by the chain dynamics may become faster than the effective partner exchange.

At high degrees of functionalization, i.e., $\epsilon > 1$, all chains are involved in the formation of a percolated network as multifunctional precursors, therefore, the strand length is much shorter than the length of precursors. The final relaxation only happens through the effective partner exchange. For the fully percolated limit realized in the bulk state of telechelic systems designed for self-healing, Rubinstein and coworkers have formulated a theory of relaxation relying on the concept of bond lifetime renormalization.[56] According to this model, the time that a free sticker should look for another available partner scales with the volume explored by a compact random walk constrained by chain connectivity before possibly going back to the old partner. Therefore, the effective partner exchange time is much longer than the actual bond lifetime of the dissociation reaction, being governed by the probability to find another open sticker.

For systems composed of long chains with multiple stickers, segments shorter than the network strand relaxes by the Rouse mechanism following monomeric friction, while longer length scales follow sticky Rouse and experience additional friction by the partner exchange of stickers. A similar classification of the relaxation regimes based on the degree of functionalization exists for entangled sticky chains.[46,52,53] At $\epsilon < 0$, the system is composed of free chains and sparse associations, whose length and dispersity increase with ϵ. Relaxation follows chain dynamics, just like unentangled sticky chains, with the exception that

the faster relaxation of free chains and short transient ones accelerate the relaxation of longer associations by the effective dilation of their confining tube. Sparse networks with long entangled strands appear beyond the gel point, i.e., $0 < \epsilon < 1$, whose break up into smaller subclusters may proceed by the faster chain dynamics. Finally, all precursors get involved in the percolated network and form multiple junctions at $\epsilon > 1$, as such, their relaxation requires several effective partner exchange steps. Therefore, segments shorter than the network strands that are defined by the combination of physical entanglements and transient junctions relax by the Rouse mechanism according to the monomeric friction, whereas longer segments up to an entanglement length relax by the sticky Rouse, experiencing additional friction coming from the reversible associations. Relaxation of segments with length scales beyond an entanglement, or diffusion on such length scales, follows chain dynamics with the same additional friction, as explained by the sticky reptation mechanism.[43,46]

3.2. Dynamics of Associative Polymers with Aggregates

A large difference between the solubility parameter of transient pairwise associations and the polymer backbone usually results in the phase separation of polar associations into large aggregates, where given the requirements they may further form ordered structures mediated through secondary interactions between associative groups, as detailed in Ref.[8] The formation of large aggregates significantly hinders the chain relaxation process.

In the simplistic view of Semenov and Rubinstein, which is in fact the only one existing so far, aggregated stickers can be considered as a dense core with polymer segments forming loops like petals in a flower-like micelle.[57,58] At high sticker concentrations, some polymer segments can bridge between micellar cores and transiently connect them. As such, a transient network with micellar junctions of long lifetime and large functionality will be formed. Therefore, on top of all parameters governing the dynamics of associative polymers, the aggregate lifetime and the number of stickers per aggregate determine the final relaxation mechanism. The number of stickers per aggregate, which
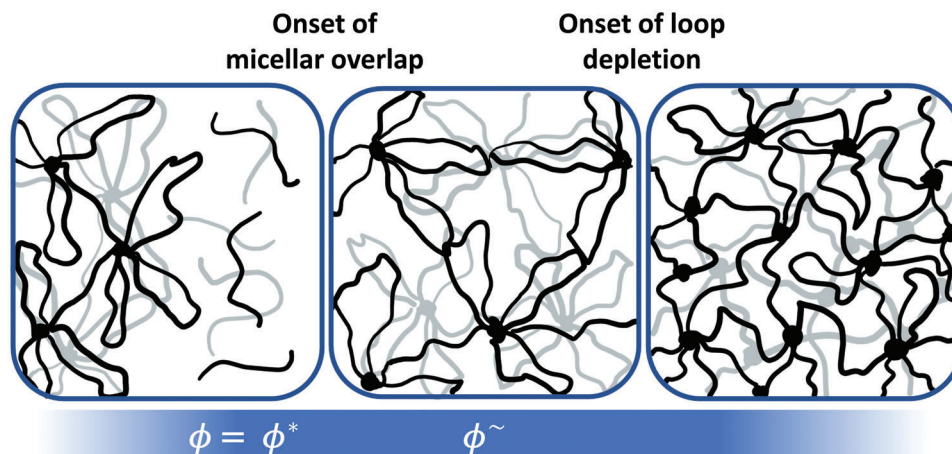
**ADVANCED
SCIENCE NEWS**

www.advancedsciencenews.com

M acro-
olecular
Chemistry and Physics

www.mcp-journal.de

Figure 3. Variation of the structure composition in associative polymers in the presence of micellar aggregates by increasing the concentration, arcing from phase-separated aggregates, to micelle overlap or gelation, and to a critical concentration when the number of bridges approaches the number of stickers per aggregate.

depends on the counter effects of the length of the polymer segments between stickers and the association energy, determines the structure of the network at equilibrium.

Semenov and Rubinstein have provided scaling laws for associative polymers that form micellar aggregates dominating the linear viscoelastic behavior. In the first variant,[57,58] telechelic chains with a linear precursor and two sticky terminal groups are considered. The association of terminal groups forms a compact core surrounded by a corona of polymer chains that form loops. The inner structure of the micelle resembles that of a star polymer with m arms, where m is also the number of stickers per micelle. Unlike stars that repel each other, micelles attract themselves in a solution due to the possibility of forming bridges. The attraction energy between two micelles scales with the number of shared bridges. This results in the macro-phase separation of micelles from the isolated chains in dilute conditions, as illustrated in **Figure 3**. The macro-phase separation fades at the micellar overlap concentration, $\phi^* \sim (\sqrt{m}/N)^{3\nu-1}$, where N is the degree of the polymerization and ν is the Flory's scaling exponent, which is 0.5 for the θ solvent and 0.59 for a good one. Micelles become progressively nonspherical and the number of bridges increases with concentration, up to a critical concentration, $\phi^\sim \sim (m^2/N)^{3\nu-1}$, beyond which loops are depleted and all chains form bridges. Chains are no longer stretched at such concentrations and therefore they connect not only neighboring but distant cores, as illustrated in Figure 3.

The stress relaxation proceeds either through the bridge exchange (or bridge-to-loop transformation), which is characterized by the energy barrier for the dissociation of a sticker from a core, B, or by the micelle rearrangement or repositioning, which is activated by the energy barrier for the formation of a free volume of the size of the micelle. The dominating mechanism depends on the number of bridges per micelle, which results in concentration-dependent scaling laws. If $B > m^{3/2}$ the viscosity increases exponentially with B at $\phi > \phi^*$. Otherwise, at all concentration regimes, the relative viscosity scales with the number of stickers per aggregate and concentration as $\ln(\eta/\eta_s) \sim m^\alpha(\phi/\phi^*)^\beta$, where the exponent α increases from $2 - 4\nu/3$ to $3/2$ as ϕ/ϕ^* goes beyond $1 + m^{\nu/3 - 1/2}$, whereas the exponent β

decreases from 0 to a negative value at $\phi/\phi^* > (1 + m^{\nu/3 - 1/2})$, and turns positive at $\phi/\phi^* > 2$. This unusual decrease of viscosity with concentration at the intermediate concentration regime is due to the decrease of the micellar rearrangement barrier as chains become less stretched at large concentrations. In contrast, the number of bridges increases monotonically with concentration and outweighs the micellar rearrangement barrier at larger concentrations.

The exponential dependence of viscosity on concentration is much stronger than previously reported power-law scaling laws for associating polymers.[44,46] It is not surprising that this effect is much stronger in the case of entangled side-chain associating polymers with many stickers per chain, i.e., $f \gg 1$, as explained by Semenov and Rubinstein.[58] Concentration regimes similar to what is already explained for telechelic chains can be imagined: at the overlap concentration, ϕ^*, micelles form a percolated network, and at $\phi^\sim$, all polymer segments become unstretched. As such, the number of bridges can be considered zero below ϕ^*, but increases with concentration until it reaches m at $\phi^\sim$. The difference with the telechelic system already discussed is that the degree of polymerization, N, should be replaced by the number of repeating units in polymer spacers between two stickers, l, for driving critical concentrations like ϕ^* and $\phi^\sim$. Two more critical concentrations are defined regarding the entanglement state: $\phi_e^* \sim (N_e/N)^{3\nu-1}$, and $\phi_e \sim (N_e/l)^{3\nu-1}$, when chains become entangled but spacers are still not, and when spacers also get entangled, respectively.

One of the elementary steps in stress relaxation would be sticker hopping by dissociation from the parent aggregate and association with another one. Due to the large functionality of micelles, and their distribution implying flexibility in the size, the energy difference between adducts and products is negligible. This means that the renormalization of the bond lifetime due to the repeated return of dissociated stickers back to their old partner was treated more recently by Stukalin et al.[56] can be neglected. Thus, the bond lifetime should largely be governed by the activation-free energy, which should include entropic contributions due to steric hindrance and stretching of the polymer spacers. Taking up the earlier work[58] again

focusing on multifunctional chains, the bond exchange process is characterized by a characteristic time that scales with the squared number of stickers, $\tau \sim \tau_b f^2$, just like the sticky Rouse mechanism, where τ_b is the sticker lifetime. The relaxation becomes much slower as chains get entangled beyond ϕ_e^*. The relaxation follows the curvilinear diffusion along the tube, with higher friction imposed by sticker hopping, therefore the general correlation between the reptation and Rouse relaxation times applies, i.e., $\tau \sim \tau_b f^2 Z$, where $Z = N/N_e$ is the number of entanglements. The loop-bridge transformation by the sticker hopping is arrested at higher concentrations, i.e., $\phi > \phi_e$, as spacers also become entangled. Therefore, stickers have to leave the tube by double-folding an entanglement strand to access the neighboring core. This results in an additional strong concentration dependence of relaxation time: $\ln(\tau/\tau_b) \sim f^3 (\phi/\phi_e)^\beta$.

However, in this case as well as for aggregate-forming telechelic chains, stress relaxation in the concentrated or bulk state is thought to require micelle deformation and repositioning of the jammed micellar suspension. This process should be dominant, as it is exponentially slower compared to sticker hopping, as to hop to a new place, a micelle should remove all bridges and relax all entanglements with old neighbors and replace them with new ones. The above-discussed timescales of chain relaxation should thus be of minor relevance for the actual flow. Below, we will discuss recent experimental evidence which actually disproved this assumption and suggested that flow in such systems is indeed governed by single-chain relaxation.

3.3. Tube-Based Models for Associative Polymers

The mean-field approach is valid where all chains have the same probability to form entanglements, binary associations, and aggregates. With that, a quantitative correlation can connect the molecular characteristics to the equilibrium structure and eventually macroscopic properties such as diffusion and dynamics. Such a correlation can be insightful for the rational design of associative polymers, or inversely to characterize their molecular specificities based on macroscopic properties.

The original tube model was introduced by de Gennes and promoted by Doi and Edwards as a quantitative tool for the prediction of the linear viscoelastic (LVE) behavior of entangled chains.[59,60] Different elements like double reptation concept by des Cloizeaux,[61] constraint release and dynamic tube dilation by Milner and McLeish[42] have been included by various algorithms to provide quantitative tube-based models like the time marching algorithm (TMA) by van Ruymbeke et al.,[40,41,62] the hierarchical model by Larson et al.,[63,64] or the branch-on-branch (BoB) model by McLeish and coworkers.[65,66] Such models can provide a quantitative prediction of LVE properties of polymer chains even with complex architectures.[66–71] The main advantage of TMA model is that it considers all relaxation processes in parallel, therefore, there is no need for the time–length separation of the involved mechanisms, as each becomes dominant at its own characteristic time.[41,72] Here we use the notation of TMA model, but similar equations can be found in other models.

The simplest approach for extending tube-based models of entangled chains to associative polymers is by considering f number of equidistantly placed stickers along the polymer chain, which can form pairwise associations:[43]

$$A + A \underset{k_d}{\overset{k_a}{\rightleftharpoons}} X \tag{1}$$

Considering large association energy, ϵ, the majority of stickers are associated at every glance.[51] The fraction of associated stickers, p, the association kinetics, the lifetime of pairwise association, τ_a, and the time that stickers are free before reassociation, τ_a, are correlated as:[43]

$$\frac{\tau_a}{\tau_b} = \frac{1-p}{p} = \frac{k_d}{2k_a [A]} \tag{2}$$

where the lifetime of a transient binary association is $\tau_b = 1/k_d$. Before the dissociation of transient crosslinks, the system behaves similarly to the equivalent permanently crosslinked network. Relaxation is halted beyond the spacing between two stickers until associations open and start to randomly exchange their partners. All relaxation processes at the timescale beyond the association's lifetime are somehow affected by the presence of stickers.[44,46]

The relaxation of polymer chains is limited to the fluctuations of bond length or oscillation of substituents at very short times or low temperatures. The permissible relaxation length increases by the observation time or by increasing the temperature so that two carbon–carbon bonds change their gauche–trans angles and the segment in between flips and changes the conformation. This process is explained by the Rouse mechanism and its specific time depends on the monomeric friction of the mobile segment.[73] The Rouse relaxation length grows to the whole chain length for short unentangled chains or long chains in dilute solutions, but it is arrested by hitting the entanglement spacing in entangled systems. From now on this relaxation mechanism is limited to one-dimensional modes along the tube axis:[74]

$$\varphi_{\text{Rouse}}(t) = \frac{1}{Z} \left[\sum_{i=Z+1}^{N} exp\left(\frac{-i^2 t}{\tau_e Z^2}\right) + \frac{1}{3} \sum_{i=1}^{Z} exp\left(\frac{-i^2 t}{\tau_e Z^2}\right) \right] \tag{3}$$

where N/i monomers change their conformations at the mode i. In the presence of binary associations, however, the Rouse relaxation is halted at a shorter length, which is defined by the average length between entanglements and transient crosslinks, and the longitudinal 1D modes are often neglected. Instead, the Rouse modes up to the entanglement spacing are activated after the dissociation of transient bonds. Nevertheless, they are slowed down due to the parallel association/dissociation, or blinking, of transient bonds, as defined by the sticky friction in the sticky Rouse mechanism:[49]

$$\varphi_{\text{SRouse}}(t) = \frac{1}{Z} \left(\sum_{i=Z+S+1}^{N} exp\left(\frac{-i^2 t}{\tau_e Z^2}\right) + \sum_{i=Z}^{Z+S} exp\left(\frac{-i^2 t}{\tau_b (Z+f)^2}\right) \right) \tag{4}$$

Reptation follows the same mechanism as Rouse relaxation, but it is limited to the contour length of the chain along the tube axis. A local loop inside the tube changes the conformation by the

**ADVANCED
SCIENCE NEWS**

www.advancedsciencenews.com

Macro-
molecular
Chemistry and Physics

www.mcp-journal.de

gauche–trans transformation of bonds at both ends and somewhere else a reverse transformation happens to keep the defined thermal energy constant as if the loop is displaced along the tube. By each random displacement, a kick in a random direction along the tube is exerted on the chain, which results in a reciprocal movement of the chain along the tube.[73] The random reorientation of external chain segments along with the reciprocal diffusion in the tube results in the removal of the memory of the original confining tube, which eventually leads to relaxation by the following reptation survival probability:[40,41]

$$p_{\text{rept}}(x.t) = \sum_{i.odd} \frac{4}{i\pi} \sin\left(\frac{i\pi x}{2}\right) \exp\left(\frac{-i^2 t}{3\tau_e Z^3}\right) \quad (5)$$

where x is the dimensionless segment position varying from 0 at the chain end to 1 at the middle of chain. In the presence of binary associations, this process is slowed down by sticky friction. Nevertheless, it is not necessary for the sticky reptation to have all stickers dissociate at once, as the reciprocal diffusion proceeds gradually through the displacement of local kinks. Therefore, it is enough to replace the characteristic disentanglement time of $3\tau_e Z^3$ by the characteristic sticky reptation time of $3\tau_b Z^2 f$.[43]

For branched chains and stars, where the branching point arrests the reptation along the tube like an anchor, retraction and expansion of branches/arms or CLF is the only possible relaxation mechanism.[42,75] This process is driven by the thermal energy for external segments and becomes exponentially slower for deeper ones that should overcome their CLF barrier. Although CLF is the only relaxation mechanism for star-like chains, simulations have proved that it has a significant contribution to the relaxation of linear chains, as well, specifically in short chains and for external segments. The corresponding CLF survival probability reads as:[40,41,62]

$$p_{\text{fluc}}(x,t) = \exp\left(\frac{-t}{\tau_{fluc}(x)}\right) \quad (6)$$

The characteristic CLF time, $\tau_{fluc}(x)$, is explained by the early and late CLF modes, the latter being slowed down by energy barrier of retraction, $U(x)$:[40,62]

$$\tau_{early}(x) = \frac{9\pi^3}{16}\tau_e Z^4 x^4 \quad \text{for } x < x_{trans} \quad (7)$$

$$\tau_{late}(x) = \tau_{early}(x_{trans}) \exp\left(\frac{\Delta U(x)}{k_B T}\right) \quad \text{for } x > x_{trans}$$
$$U(x) = 3k_B T Z \int_0^x s(1-s)^\alpha ds \quad (8)$$

The transition between the two CLF modes happens at a segment where the CLF penalty equals the thermal energy ($U(x_{\text{trans}})$ = $k_B T$). The CLF process should be accordingly slowed down by the sticky friction just like the sticky reptation. This can be taken into account simply by updating the friction term in the definition of τ_{early}:

$$\tau_{early}(x) = \frac{9\pi^3}{16}Z^2\left(\tau_e Z^2 + \frac{2}{3\pi^2}f\tau_b Z\right)x^4 \quad (9)$$

But the concept of sticky CLF has been rarely used as sticky reptation is much faster for deeper segments and therefore governs the terminal relaxation of associative chains.[76,77] However, further experimental evidence should be provided to check if the sticky CLF as defined here governs the relaxation of highly-branched and star-like associative polymers. The TMA model determines the fraction of oriented chain segments by summing up the ones that are not relaxed by the reptation or the CLF processes:[40]

$$\varphi_{\text{chain}}(t) = \int_0^1 p_{fluc}(x.t)\, p_{rept}(x.t)\, dx \quad (10)$$

Accordingly, the transient modulus is calculated based on the fraction of oriented chain segments, the fraction of oriented tube segments, and the high-frequency Rouse (or sticky Rouse) modes:[40]

$$\frac{G(t)}{G_N^0} = \varphi_{(S)\text{Rouse}}(t) + \varphi_{\text{chain}}(t)\,\varphi_{\text{tube}}(t)^\alpha \quad (11)$$

where the dilution exponent, α, takes a value between 1 and 4/3.[78,79] Following the mean-field approach, the fraction of oriented tube segments is determined from that of chain segments by a relaxation rate not faster than what the Rouse relaxation mechanism allows:[40,42]

$$\varphi_{\text{tube}}(t_i) \geq \varphi_{\text{chain}}(t_{i-1})\left(\frac{t_{i-1}}{t_i}\right)^{0.5} \quad (12)$$

Moreover, along with time, the already relaxed segments dilate the confining tube of still-oriented segments just like a solvent, according to the dynamic tube dilation, which is taken into account by updating the number of entanglements at each time step:[40,42]

$$N_e(t) = N_e(0)\,\varphi_{\text{active}}(t)^\alpha \quad (13)$$

where the fraction of already relaxed chains, φ_{active}, which can be felt by every relaxing chain depending on the length of the chain, as longer chains have a longer lag time to feel the environment following to Graessley's criterion:[40,80]

$$\varphi_{\text{active}}(t) = \varphi_{\text{tube}}(t/Z^2) \quad (14)$$

Of course, the constraint release and dynamic tube dilation are physical processes independent of the presence of stickers, however, they are equally slowed down parallel to the hindrance of the relaxation of the probe chain. Accordingly, the tube-based model provides a universal behavior for the relaxation of associative polymer chains. This behavior is adjusted to the timescale and flexibility of each polymer by the material parameters, τ_e, N_e, and G_N^0 for non-associative chains and with additional material parameters of f and τ_b for associative ones.

Tube-based models can be similarly extended to the case of telechelic associating polymers.[81–83] They treat transient chains as permanent equivalents below the dissociation time of stickers. Above the dissociation time, however, either a Monte Carlo algorithm should be developed to account for the dynamic shuffling of living chains,[84] or simply the terminal relaxation should be
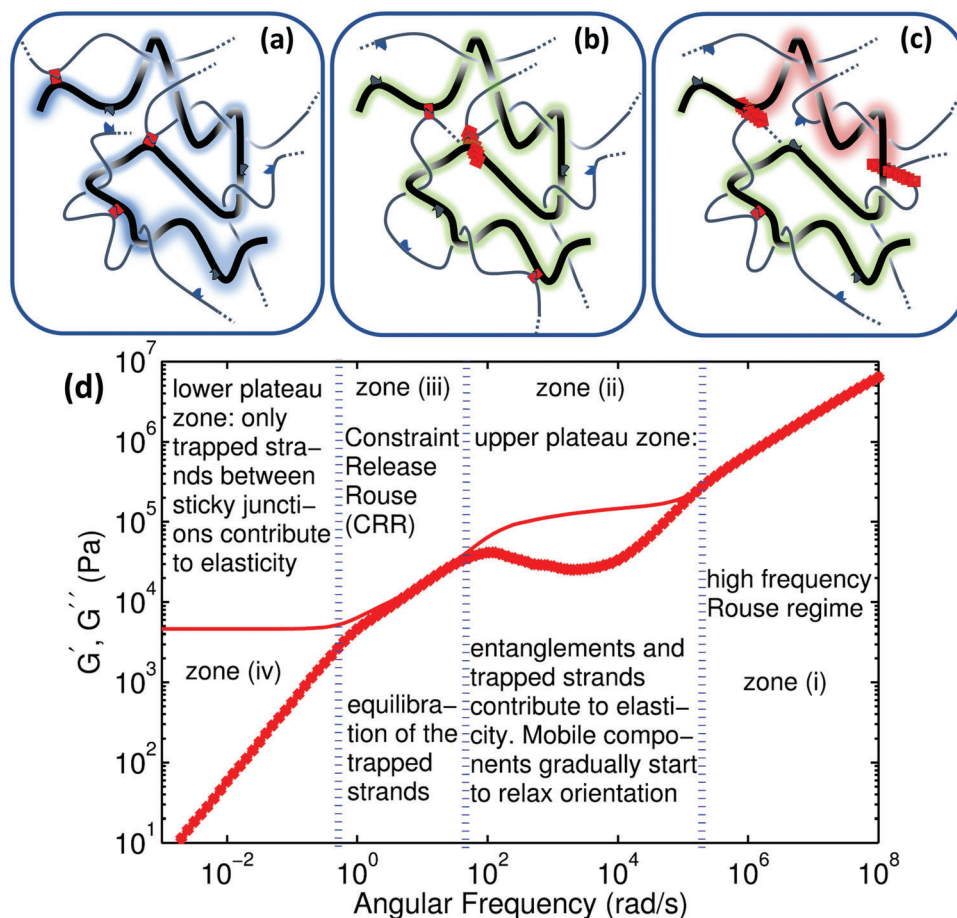
ADVANCED
SCIENCE NEWS
www.advancedsciencenews.com

{M} acro-
olecular
Chemistry and Physics
www.mcp-journal.de

Figure 4. Mobility of chain segments in the presence of clusters: a) cluster-free chains capable of sticky reptation, b) chains contributing in just one cluster capable of sticky CLF, c) chains contributing in more than one cluster contain dangling ends capable of sticky CLF, and immobile trapped segments (highlighted in red) that connect stable clusters. Adapted with permission.[6] Copyright 2019, American Chemical Society d) graphical illustration of the four relaxation regimes (zones) considered in the model. Adapted with permission.[85] Copyright 2016, American Institute of Physics.

considered, following the individual relaxation of dissociated precursors. This might be a rough estimate in many cases as chains may reassociate before the complete relaxation.[82,83]

3.4. Tube-Based Models for Associative Polymers with Aggregates

Polymer chains are normally formed by statistical polymerization methods that end up in a specific distribution of chain length and chemical composition. Associative polymers, on top of that, are usually formed by statistical post-polymerization modification techniques, which result in an additional dispersity of the microstructure. Therefore, the association tendency, which depends on the spacer length, and the number of neighboring sticky groups, change from chain to chain, which results in a distribution of the equilibrium number of stickers per aggregate. However, the thermodynamic equilibrium structure is also hindered by the slow kinetics of phase separation specifically in well-entangled polymers. Therefore, the ideal picture of associative polymers with ordered micellar aggregates, as discussed in Section 3.2, is often far from reality. The real system is often

composed of chains with pairwise associations, contributing in n number of aggregates, or collective assemblies, where $0 \leq n < f$. Therefore, the application of the mean-field approach, where the probe chain represents the environment, is also impossible. Instead, a simplified approach would be to classify associative chains into cluster-free ones, which relax by the sticky reptation mechanism, chains contributing only in one cluster, which relax by the sticky CLF mechanism like an associative star chain, and chains contributing in more than one cluster, which are composed of dangling end segments that relax by the sticky CLF and internal segments that are incapable of relaxation, as illustrated in **Figure 4**. The environment is consequently built by the contribution of each class in tube relaxation.

Van Ruymbeke and coworkers have developed such a statistical model to predict the LVE properties of randomly hydrolyzed poly(n-butyl acrylate) (PnBA) chains, which show strong phase separation specifically at large degrees of hydrolysis.[6,85] Segments located between two clusters are considered trapped and the rest of polymer segments are considered mobile. The relaxation of mobile segments follows monomeric friction by ignoring the presence of pairwise associations.[85] Whereas the relaxation of trapped chains is explained by the constraint release Rouse pro-
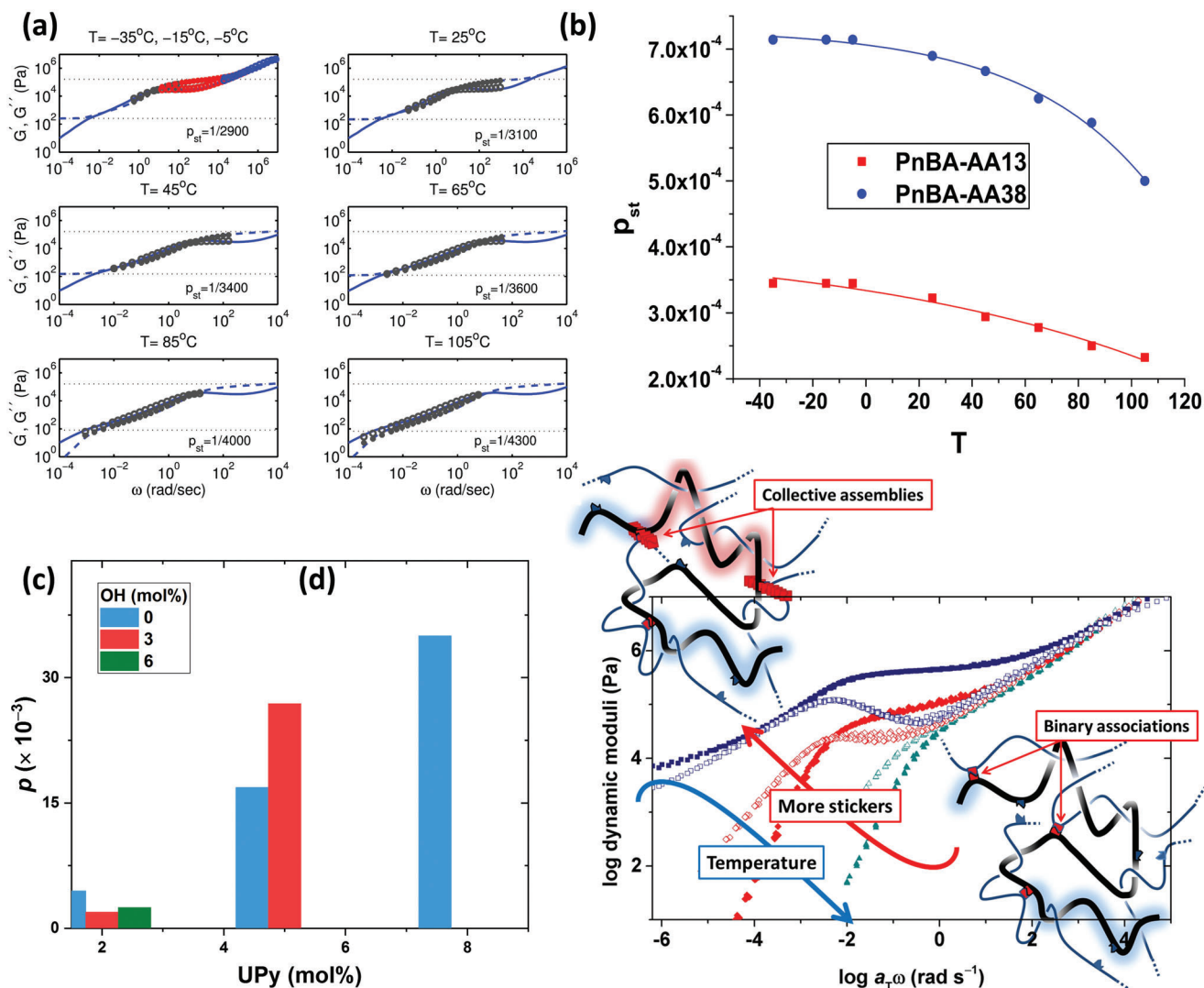
**ADVANCED
SCIENCE NEWS**

www.advancedsciencenews.com

**Macro-
molecular**
Chemistry and Physics

www.mcp-journal.de

Figure 5. Effect of temperature on a) dynamic moduli of PnBA chains with 38% hydrolyzed repeating units and b) the fraction of cluster-forming monomers for samples with 13% and 38% hydrolysis. Adapted with permission.[85] Copyright 2016, American Institute of Physics. c) Effect of sticker (UPy) content on the mean-field penalty of CLF of PnBA chains that also carry comonomers with free hydroxyl groups as denoted in the legend. Adapted with permission.[86] Copyright 2022, American Chemical Society. d) Cartoon representation of the effect of increasing the temperature (corresponding to panels a and b) or sticker content (corresponding to panel c) on the fraction of aggregates. Adapted with permission.[6] Copyright 2022, American Chemical Society.

cess (CRR), which allows trapped segments to occupy a dilated tube following a Rouse-like mechanism, after the relaxation of mobile segments, as illustrated in Figure 4d. As the phase separation results in severe thermorheological complexity, the construction of master-curves and the application of the resulting tube model to the whole time/temperature domain are not possible. Instead, the application of the model on the LVE data obtained at each temperature is very insightful in revealing the fraction of cluster-forming monomers and its temperature dependence, as shown in **Figure 5**a,b. We have also recently proposed a very crude approach by considering all chains contributing in both pairwise and collective assemblies and replacing the effect of clustering with a mean-field penalty that equally applies to all chains.[86] As such, we ignored the sticky reptation and explained the relaxation of mobile segments by a CLF process that is hindered by

the mean-field penalty:[86]

$$p_{\text{fluc}}(x,t) = \exp\left(\frac{-t}{p\tau_{\text{fluc}}(x)}\right) \tag{15}$$

where the relaxation penalty, p, equals one in the absence of stickers and increases with the introduction of stickers, and clusters, accordingly, as shown in Figure 5c. Both approaches, i.e., the tube-based model of van Ruymbeke and our crude empirical approach, do not consider any relaxation associated with clusters,[6,85,86] i.e., the cluster disintegration by sticker hopping and the cluster hopping and repositioning.[58] The aggregates are reflected as permanent junctions, where the fraction of segments trapped between them form a low-frequency plateau as represented in Figure 5d. Therefore, they are independent of the clus-

**ADVANCED
SCIENCE NEWS**

www.advancedsciencenews.com

{M} acro-
molecular
Chemistry and Physics

www.mcp-journal.de

ter specificities, such as the number of stickers per aggregate or aggregation tendency. Although this is obviously a shortcoming, it is not surprising as systematic information regarding the cluster dynamics and its correlation to the microscopic characteristics, i.e., energy and number of associations per aggregate, is still lacking. Therefore, further systematic experimental studies and application of hybrid modeling approaches that include the network junction functionality, like Miller-Makosco's model of network percolation could be very enlightening.[55,87]

4. Experimental Insights

The alteration of thermal, dynamic, and mechanical properties of supramolecular polymers upon aggregation and clustering often stems from the variation of the structure and morphology. The structure alteration is frequently characterized by scattering techniques specifically small angle X-ray (SAXS), and light scattering (LS), besides direct observation by microscopy techniques.[8] The consequent variations of properties are often characterized by thermal analysis, broadband dielectric spectroscopy (BDS), and rheology. The application of these techniques in characterizing clustering is recently reviewed elsewhere.[8] Therefore, our focus here is solely on the dynamics of sticky chains in presence of clusters and the dynamics of clusters themselves. Although many reports are available on this topic, several discrepancies can be found in the provided results and conclusions. This is not surprising, given the various modes and regimes of aggregation on top of the inevitable structural dispersities in polymeric systems, as discussed in Section 3. Consequently, drawing a general picture based on the available experimental records that are comprehensively applicable to all supramolecular systems is challenging. However, most inconsistencies might be avoided by focusing on the correlation between the structure and properties of supramolecular materials rather than targeting the correlation of design parameters and consequent dynamics in individual chemistries or polymer topologies.

4.1. Structure and Morphology of Aggregates in Associative Polymers

Without clusters, the extra friction on chain dynamics induced by transient associations is the main parameter that alters the dynamics of the whole system. In the presence of clusters, however, phase-segregated nanodomains formed by the associative groups define the final morphology and mainly determine the consequent dynamics. Therefore, in the following, we first categorize literature reports on cluster-forming supramolecular materials in three possible morphologies and then try to explain available experimental records on dynamic properties, accordingly.

4.1.1. Well-defined, ordered aggregates

Well-defined ordered aggregates have been mostly reported when unentangled backbones are used, specifically with monofunctional precursors.[26,27,35,88–92] The association of end groups in mono-functional telechelic precursors forms transient dimers,

which further associate via secondary interactions and make an ordering that resembles the structure of ABA block copolymers ranging from micellar to fibrillar and lamellar morphologies depending on the network composition.[93–95] SAXS is often served to confirm specificities of the distinct morphology.[95,96] Nevertheless, their dynamic properties are often similarly affected by such an ordering. Unentangled poly(isobutylene), (PIB) end-functionalized with 2,6 diaminotriazine (Tr) is a good example, whose SAXS pattern confirms the body-centered cubic sphere (bcc) structure below ordered disordered transition temperature (ODTT) of 110 °C.[26,27] The middle block of the pairwise homocomplementary associations from different chains aggregate together and form dense cores by a shell of nonpolar polymeric blocks. These spherical micelles then pack into an ordered bcc nanostructure. Similarly, SAXS and atomic force microscopy patterns of PnBA chains with 40 kg mol⁻¹ molar mass that are centered and functionalized with strong triurea groups indicate the organization of nanofibers, which are hexagonally packed in oriented nanodomains.[97,98] The aggregation of strong UPy groups into fibrillar structures has been also reported for several telechelic supramolecular materials.[89,99,100] Metallo-supramolecular polymer networks are reported to form well-defined ordered aggregates with various morphologies, likewise, as shown in **Figure 6**a, for the case of terpyridine (TPy)-functionalized unentangled poly(butadiene) (PBd) precursors associated with Zn^{2+} metal ions.[95,101] To provide a lucid comparison with other structures, key dynamics and rheological features of this class of materials are summarized as follows:

Below the ODTT, the material reveals a broad plateau modulus caused by the interpenetration of precursor chains surrounding cluster cores, as shown in Figure 6b. Such a plateau is also observed for block copolymers with gyroid or bcc structures before the flow regime.[94] Moreover, the terminal relaxation time, determined by the crossover of storage, G′, and loss moduli, G″, and the associated zero-shear viscosity are often inaccessible. Nevertheless, the formation of the ordered structure significantly increases the viscosity, e.g., the formation of micellar aggregates is reported to increase the viscosity 33 times of the nonfunctionalized PIB.[27]

4.1.2. Well-Defined, Non-Ordered Aggregates

In this case, the phase separation of associative groups results in aggregates with defined morphologies, however, they cannot form an ordered structure. One example is the telechelic Tr-PIB mentioned in the previous section above its ODTT, or also thymine-functionalized PIB (Th-PIB).[26,27] Despite the association constants of Tr and Th being comparable, the fraction of clusters in the case of Th-based polymer is not sufficient to form an ordered structure, as revealed by SAXS measurements. This might be related to the different molecular structures of Tr and Th motifs. Similarly, the heterocomplementary 1:1 mixture of Tr-PIB and Th-PIB indicates a micellar structure but without a strong ordering, as also illustrated in Figure 6b. A lamellar structure is actually reported when Th end groups of poly(propylene oxide) (PPO) precursors aggregate and crystallize. The crystallization is avoided when complementary Tr-functionalized precursors are introduced, however, due to the polarity of the PPO backbone,
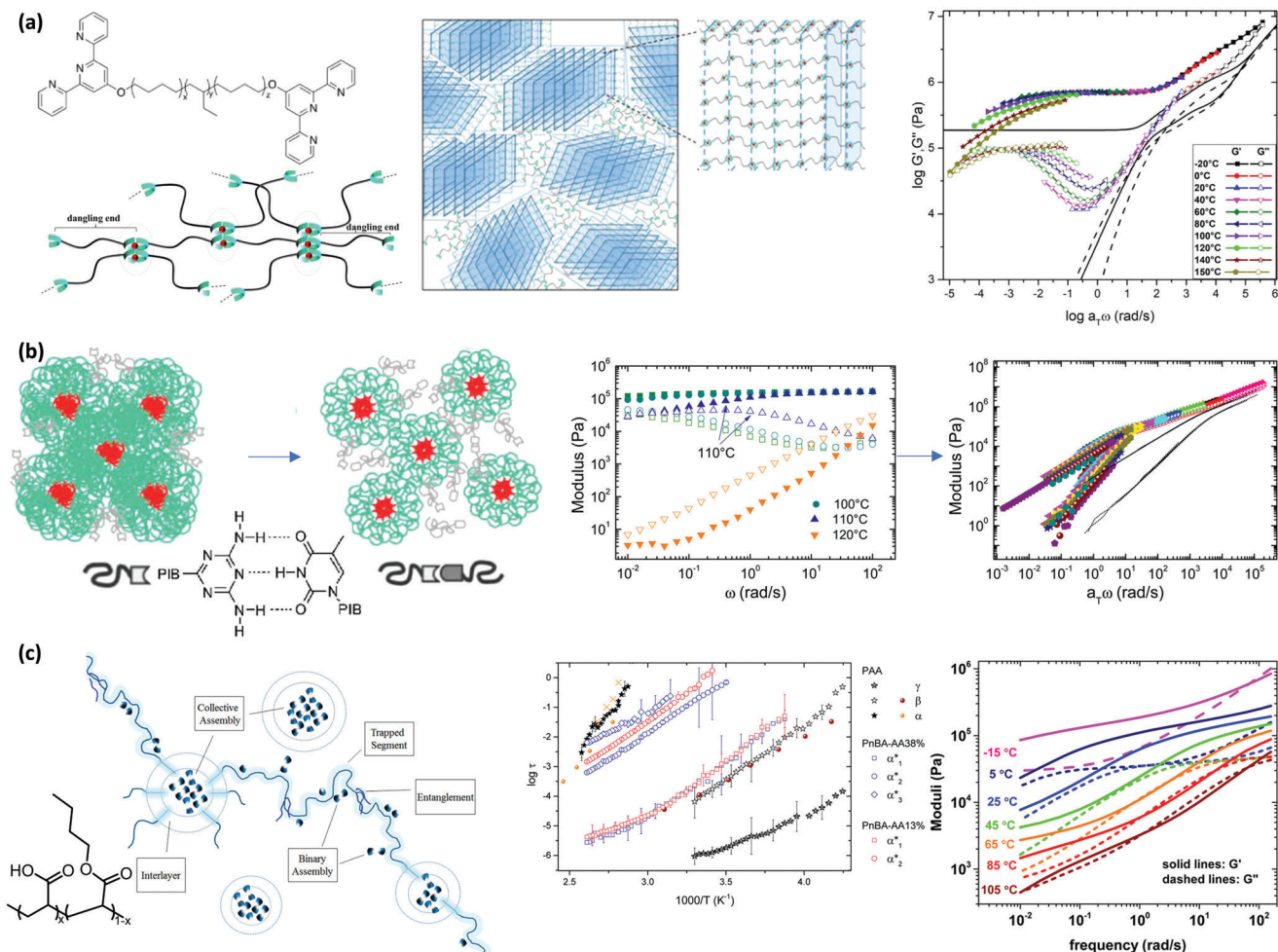
ADVANCED
SCIENCE NEWS

www.advancedsciencenews.com

Macro-
molecular
Chemistry and Physics
www.mcp-journal.de

Figure 6. Chemical structure, morphology, and representative properties of associative polymers in the presence of aggregates: a) Well-defined order aggregates, the case of TPy-functionalized PBd showing a plateau modulus above ODTT. Adapted with permission.[95] Copyright 2021, American Chemical Society. b) Well-defined non-ordered aggregates, the case of switching from unentangled homocomplementary mono-functional Tr-PIB to heterocomplementary bi-functional Tr-PIB/Th-PIB that causes the plateau modulus to disappear, as demonstrated in the corresponding dynamic moduli. Adapted with permission.[27] Copyright 2014, American Chemical Society. c) Ill-defined non-ordered aggregates, the case of randomly hydrolyzed entangled PnBA, which show relaxations in BDS that coincide with that of PAA (middle), confirming the presence of AA-rich domains resulting in the emergence of a plateau modulus and severe thermorheological complexity (right). Adapted with permission.[111] Copyright 2016, American Chemical Society.

pairwise associations are even incapable of phase separation and micelle formation.[102] Therefore, the formation of the ordered structure is quite sensitive to the aggregation tendency, the chain length, and the entanglement of the precursor, consequently, it is often avoided by the compromise of kinetic and thermodynamic factors. In general, the key elements of the dynamics and rheological properties of such materials are as follows:

No plateau modulus is observed for unentangled precursors. Instead, samples reveal typical Rouse-like relaxation behavior, as shown in Figure 6b. Nevertheless, the terminal relaxation time is longer than that of nonfunctionalized precursors, and the associated zero-shear viscosity is higher. The increase in viscosity is larger than what is expected based on the increase of the molar mass caused by the pairwise association of supramolecular units. However, this increase is much lower than what is observed for equivalent samples that form an ordered structure, e.g., just 5

times the nonfunctionalized PIB, in the case of Th-PIB that lacks order.[27]

The temperature dependence of viscosity is much stronger than that of nonfunctionalized PIB due to the instability of clusters at high temperatures. The mechanism of the terminal flow is therefore based on chain dynamics, similar to the nonfunctionalized PIB, but with some hindrance due to the presence of associations. Nevertheless, the power law scaling of storage and loss moduli with frequency in the flow regime eventually follows the Maxwell model prediction.

The works on the Tr- and Th-modified PIBs, comparing mono- and bifunctional telechelic chains, where only the latter can form elastic bridges, teach a few relevant lessons.[26,27] In the monofunctional case with no bridges (for Tr-PIB above the ODTT as well as for Th-PIB and their mixture), the viscosity is found to be governed largely by the temperature-dependent micellar

2200389 (12 of 20)

**ADVANCED
SCIENCE NEWS**

www.advancedsciencenews.com

**Ⓜacromolecular
Chemistry and Physics**

www.mcp-journal.de

size following well-established principles of colloid physics, being described by the Krieger-Dougherty relation. In contrast, a jammed colloidal gel is formed below the ODTT. For bifunctional telechelic chains, elastic bridges form also above the ODTT, thus the viscosity increases by orders of magnitude and a plateau modulus appear. The low-frequency end of the rheological response now resembles that of a Maxwell fluid, albeit with broadened features related to a significant relaxation time distribution.[27,103] The magnitude of the plateau modulus is now not governed by a jammed colloidal gel (as for Tr-PIB below the ODTT), but is well in line with predictions based on entropic elasticity, yet including the consideration of the hydrodynamic (= volumetric) reinforcement effect of the micelles acting as filler. Insights into the mechanism of long-time relaxation and flow will be discussed in Section 4.2. We here just note that flow seems to take place without complete dissolution of the whole aggregates.

4.1.3. Ill-Defined, Non-Ordered Aggregates

Most of the literature reports on supramolecular samples with different topologies including bi- and multi-functional telechelic, or side-chain systems are emplaced in this class, in which ill-defined interconnected aggregates form along with prevailing pairwise associations, which collectively form a disordered hierarchical network-like structure. In this case, a rubbery plateau modulus is often observed even for unentangled samples. The relaxation is rather broad and multi-step resulting in an ill-defined flow regime, however, in most cases relaxation begins as soon as pairwise associations start to break.

A series of studies reported by Stadler and coworkers, in which dynamics and rheological properties of supramolecular materials with transient network structures are systematically investigated, might be placed in this group.[104–109] In a pioneering work,[106] entangled PBd precursors were randomly functionalized with urazole derivative groups. Upon modification, the width of the rubbery plateau was increased and the transition from the rubbery plateau to the flow regime was broadened. In addition, the viscosity increased and the transition from non-Newtonian to Newtonian behaviors was shifted to lower frequencies. Moreover, the power-law scaling of the storage and loss modulus with frequency became smaller. All of these effects were enhanced by increasing the degree of modification. Nevertheless, since the minor effect of urazole groups on the plateau modulus was not comparable with their significant influence on viscosity, the authors concluded that the modification of PBd chains mainly results in a significant increase of the apparent molar mass rather than the formation of a network. The authors believed that the obtained viscoelastic picture was consistent with the perception of a side-chain multifunctional precursor, where through the association, large but reversible, branched soluble clusters of transient chains are formed. This structure was replaced with a percolated network in case hydrogen bonding motifs capable of forming ternary transient bonds with two other partners were used.[108] Similarly, Stadler and coworkers investigated the relaxation of long PBd chains functionalized with a new phenyl urazole motif using BDS.[109] The results showed that the presence of associative groups induces an additional relaxation process (α^*) appearing at lower frequencies compared to the glass transition temperature, α process of the unmodified counterpart. In contrast to the α process, the intensity of α^* decreased upon increasing temperature. Accordingly, α^* was assigned to the local complex dynamics resulting from the dissociation and reformation of pairwise associations. This process was slowed down by increasing the degree of modification, however, with a rate faster than what was expected from the shift of T_g. This can be explained by the larger stability of network junctions at higher degrees of modification, which is already reported for ionomers that rely on the clustering of junctions.[108,109]

Quite similar effects are reported for random copolymers of poly(n-butyl acrylate-co-acrylic acid) with acrylic acid contents of up to 38 mol.%,[110] as shown in Figure 6c. For the sample with the highest acrylic acid content, a parallel drop of storage and loss moduli versus frequency with the slope of ≈ 0.5 on the log–log plot was observed, which was attributed to the constrain release Rouse mechanism, as discussed in Section 3.3.[85] In addition, a second plateau emerged because polymer segments that are located between two stable clusters are incapable of complete relaxation.[111] One should distinguish between this second plateau and the one that is observed for supramolecular materials with the ordered structure.[26,94] Moreover, the quantitative agreement between the relaxation modes of the BDS relaxation spectra of pure poly(acrylic acid) (PAA) and the hydrolyzed copolymer suggested that acrylic acid units phase-separate and form nanodomains with distinct T_g values embedded in a the pure PnBA matrix.[111]

A systematic study on the diffusion of sticky chains and rheological properties of (metha)acrylate polymers functionalized with UPy groups also confirmed the presence of trapped (apparently immobile) segments, slowing down the sticky chain diffusion, postponing of the storage and loss moduli crossover, and forming of a low-frequency second plateau upon clustering of UPy groups.[112–115] Many parameters including the compromise of kinetics and thermodynamics affect the rheological properties of supramolecular materials that form ill-defined nonordered aggregates. Nevertheless, to compare their dynamics with other groups that contain well-defined aggregates the key rheological properties are listed below:

A plateau modulus emerges upon functionalization even for unentangled samples. The terminal relaxation time, which corresponds to the zero-shear viscosity, is observed at much longer times compared to the unfunctionalized precursor in the case unstable clusters form. Otherwise, a second plateau emerges at low frequencies, whose intensity can be attributed to the fraction of bridge segments that connect clusters. Accordingly, the zero-shear viscosity is much higher than expected, due to the significant increase in the apparent molar mass, therefore, it is rather inaccessible even at high temperatures before the thermal decomposition. Moreover, in the presence of stable clusters, the flow activation energy or the temperature dependency of viscosity is similar to or just slightly stronger than that of unfunctionalized precursors. Simply said, the temperature dependency of dynamics of associative chains approaches that of unfunctionalized precursors upon the formation of stable clusters.

As clusters become stable, the power-law scaling of storage and loss moduli with frequency deviates from the prediction of the Maxwell model. In extreme cases, the G' and G'' drop in parallel with the slope of 0.5 on the log–log plot until the emergence

ADVANCED
SCIENCE NEWS
www.advancedsciencenews.com

Macro-
molecular
Chemistry and Physics
www.mcp-journal.de

of the low-frequency plateau. This could be considered a sign of gel structure or might be attributed to the CRR relaxation as discussed in Section 3.4.

Of course, depending on the numerous parameters that can be varied in designing associative polymers with aggregates, which arc from chemical characteristics mainly influencing the aggregation tendency, to physical specifications, like chain topology, entanglement, and sticker positioning, various dynamic behaviors are expected. However, the reported general behavior of various samples fits the abovementioned classification based on the correlation between the morphology of aggregates and dynamics. Nevertheless, there are several considerations, as discussed below, that should be taken into account before interpreting the correlation between the morphology of aggregates and the observed dynamics.

4.2. Aggregate Dynamics

Despite aggregates contributing to the plateau modulus like a multi-functional network junction, their contribution is often outweighed by the prevailing number of pairwise associations in polymeric systems with ill-defined aggregates.[6,16,17,86] In contrast, the dynamics at low-frequency region or long times is often regarded as an indicator of the formation and stability of aggregates. Three different types of behavior may emerge at low frequencies:

For the case of unstable clusters,[26,27] i.e., clusters that disintegrate by sticker hopping before the terminal flow is realized by the chain dynamics, and for associative polymers without aggregation, the standard drop of storage and loss moduli with frequency with the slopes of 2 and 1 on the log–log plot, respectively, is observed; despite the presence of associative groups postpones the crossover frequency according to the sticky Rouse and sticky reptation mechanisms, for unentangled and entangled chains, respectively.

Deviations from the Maxwellian behavior can be simply reflected as a shallow power-law scaling, which is frequently associated with the polydispersity of precursor polymers as it was confirmed by comparing transient networks based on the polydisperse poly(N-isopropyl acrylamide) and monodisperse PEG precursors.[116] Another reason could be the non-random distribution of associative groups along the polymer backbone in the case of side-chain supramolecular polymers.[110,117] The dispersity in molar mass and chemical composition distribution can also amplify inhomogeneities like loops, dangling ends, higher order connectivities, and dispersity in cluster size and stability, all resulting in broad crossover and drop of moduli with shallower slopes.[6,85]

In the case of stable clusters, the crossover of the dynamic moduli may not be experimentally accessible. After the dissociation of pairwise assemblies, a parallel drop of moduli versus frequency is often followed by the emergence of the low-frequency plateau. This effect is similar for both entangled and unentangled chains that form bridged aggregates.[6,86,115] In the case of ordered micellar structures, this plateau is attributed to an order similar to what is observed for block copolymers.[26,27,94] In the absence of orders, this plateau is attributed to the fraction of bridging chains.[111,115]

As such, the stability of clusters is an important factor in defining the dynamics of associative polymers in the presence of aggregates, specifically at low frequencies. Experimental and theoretical studies on the stability or dynamics of clusters in associative polymers, either through repositioning or rearrangement are rare. This is not surprising as distinguishing the intra-cluster dynamics from sticker dissociation is not trivial in practice. Moreover, the theoretical study of the dynamics of associative chains in the presence of clusters, specifically for the close-to-practice case of entangled backbones is overwhelming. Eventually having both accomplished, comparing an experimental study of associative polymers with numerous structural dispersities with a theoretical study based on a monodisperse system, specifically with a defined number of stickers per aggregate may not be helpful.

Saalwächter and coworkers studied the aggregation in supramolecular systems with various topologies including ionomers with an entangled side-chain functionalized precursors or with unentangled bifunctional telechelic backbones, as well as three- and four-arm telechelic precursors with hydrogen bonding end groups.[103,118,119] All these systems are governed by entropic elasticity of the chains bridging the clusters. The focus of their study was on comparing the chain dynamics as revealed by a dedicated NMR relaxometry technique (MQ-NMR), reflecting single-chain relaxation, with other methods like BDS and dynamic mechanical analysis (DMA, rheology), which reveal motions of the stickers and bulk relaxation, respectively. This allowed them to detect various relaxation mechanisms and compare single-chain and terminal relaxation dynamics. In all studies, the timescale of the relaxation process found by MQ-NMR coincides well with those found by rheology, as shown in **Figure 7**a. This implies that chain dynamics is responsible for terminal relaxation. Thus, micellar rearrangement and repositioning as advocated by Semenov and Rubinstein,[58] which requires all stickers to dissociate, or all the bridging segments to relax, respectively, which requires much longer relaxation time, is not necessary. Instead, the validity of sticky Rouse and sticky reptation mechanisms even for supramolecular systems in the presence of aggregates are suggested. The authors concluded that the terminal relaxation of these systems is mainly controlled by the association lifetime, which depends on factors relevant to leaving the cluster and to translational motion through the polymer matrix.

In addition, the BDS results demonstrate a relaxation process with a timescale between that of segmental motion and terminal relaxation, which is most probably related to the motions of end groups within clusters, i.e., the intra-aggregate rearrangement. Notably, this relaxation has a temperature dependence similar to that of the sticker-related chain modes and has consequently been associated with the local sticky bond lifetime, possibly subject to lifetime renormalization[56] discussed above in Section 3.1.[120–122] However, in the given study the variation across the sample series with variable alkyl tail length of the sticky group (tuning their association lifetime) is opposite to that of the chain modes. The timescale separation of sticker-related and chain modes as explained by lifetime renormalization should depend on the sticker separation along the polymer chain, yet cluster sizes and their separation are all of comparable magnitude in the given sample series. The opposing trends across the sample series thus rule out that this model can be applied. The results suggest that the association lifetime and the timescale of
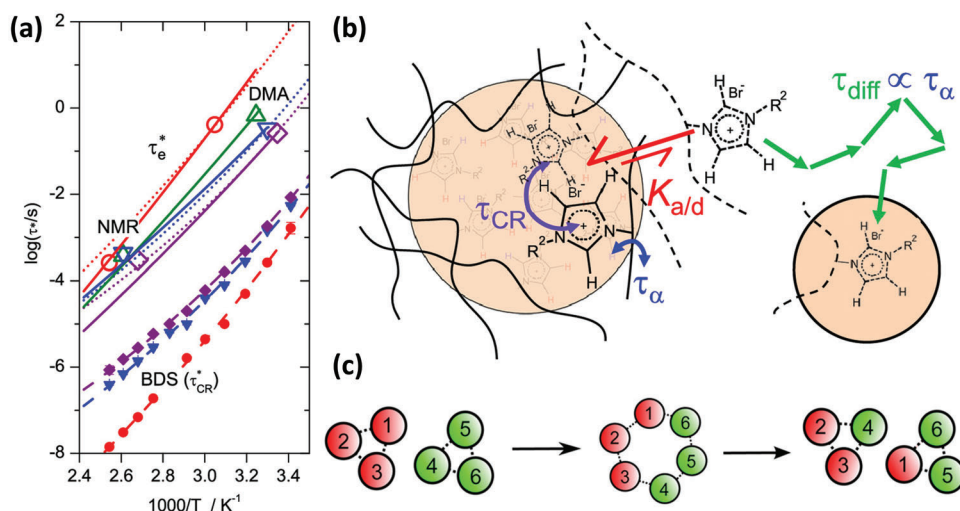
ADVANCED
SCIENCE NEWS

www.advancedsciencenews.com

Macro-
molecular
Chemistry and Physics
www.mcp-journal.de

Figure 7. a) Comparison of the timescale of relaxation processes found by MQ–NMR with ones found by DMA as well as cluster-related relaxation times from BDS for butyl rubber functionalized with ionic alkylimidazolium bromide groups with variable pending alkyl group lengths (methyl = red to nonyl = purple), which tune the bond lifetime: NMR and rheology data confirm single chain relaxation governs the terminal relaxation, whereas BDS detects a much faster relaxation associated with the intra-aggregate rearrangement b) Illustration of the proposed hierarchical relaxation of sticky chains with clusters: segmental process (τ_α), cluster relaxation process (τ_{CR} controlled by association/dissociation equilibrium, $K_{a/d}$), and diffusion of sticky chain through the polymeric matrix (τ_{diff}), which itself depends on the segmental motion. Adapted with permission.[118] Copyright 2019, American Chemical Society c) Illustration of the partner exchange of cluster mediated through sticker dissociation—association. Adapted with permission.[51] Copyright 2016, American Chemical Society.

intra-aggregate relaxation may to a degree be independent of each other, in other words, the factors governing the relation of intra-aggregate motion detected by BDS and the actual bare bond lifetime (residence time in the cluster) remain unexplained. Since the activation energies of all processes are rather similar, entropic factors likely play a key role.

Considering all of these results, the authors proposed a hierarchical relaxation process for sticky chains with clusters including segmental relaxation, cluster relaxation (controlled by association/dissociation equilibrium), and diffusion of sticky chains through the polymeric matrix, which itself depends on the segmental motion, as schematized in Figure 7b. In contrast, Gold et al. assigned the relaxation of unpolar poly(isoprene) chains functionalized with Stadler's urazole-based hydrogen-bonding groups observed in BDS spectra to the mean lifetime of the pairwise associations and correlated it to the relaxation observed in rheology.[121] This was taken as the first experimental proof of the lifetime renormalization model.[56] In view of the later results discussed above, this conclusion appears questionable, in particular, because that model is strictly limited to pairwise associations, where partner exchange requires the encounter with another open sticker, which is a rare event. In view of the work of Stadler,[104–108] cluster formation can actually not be excluded in the system of Gold et al., and a critical evaluation of the simple telechelic polymers studied by the Sokolov group[120,122] should also consider the possibility of clustering.

From the theory side, Amin and coworkers developed a molecular dynamics/Monte Carlo simulation to study the dynamics of unentangled telechelic associative polymers with sticker functionality of 3, which form clusters with a finite number of stickers per cluster. The cluster size is determined by the counter effects of energy gain and entropic penalty raising by stretching

of polymer chains, therefore, it grows exponentially with association energy.[51] They proposed a so-called partner exchange mechanism for the terminal relaxation that occurs by the combination of two close clusters and subsequent breakage into two new ones, as illustrated in Figure 7c. The characteristic time of this process increases exponentially with the bonding energy and is up to two orders of magnitude larger than the lifetime of a pairwise association. The partner exchange has a much lower energy barrier compared to the alternative sticker hopping process, in which the dissociated sticker from a cluster or micelle core should diffuse as an open sticker until finding another cluster to associate with. Moreover, the authors proposed that large clusters can facilitate polymer chain relaxation by promoting the partner exchange process. The determined $G(t)$ clearly showed that preventing the sticker clusters from growing in size leads to much slower stress relaxation in comparison with supramolecular networks with larger clusters.

4.3. Time–Temperature Superposition

Generally, the time–temperature superposition rule (tTs) should not be valid in supramolecular materials, since an additional relaxation process associated with transient bonds on top of those connected with dynamics of unfunctionalized precursors should occur along with screening dynamic properties. If the temperature dependency of the additional supramolecular relaxation is different from that of chain relaxation, this can result in the violation of the tTS rule. Thus, using tTS in a limited time–temperature range should reflect the temperature dependency of the relaxation process that dominates that specific time/temperature regime.[123] This way, many researchers have
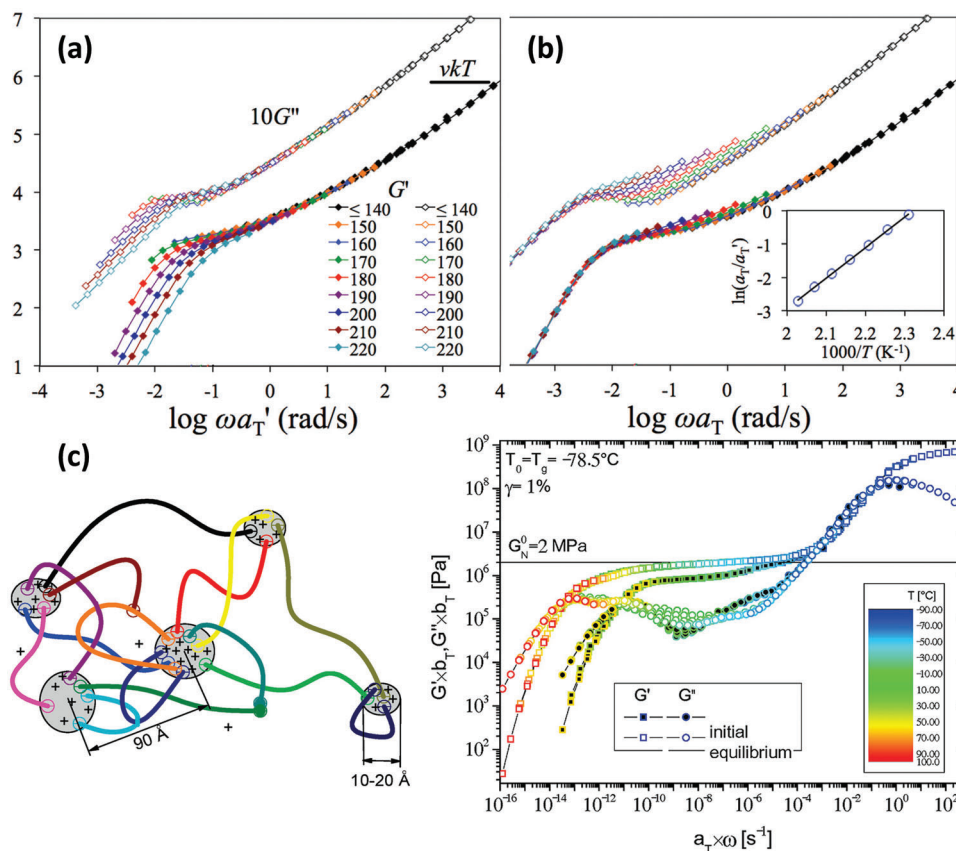
ADVANCED
SCIENCE NEWS
www.advancedsciencenews.com

[M]acro-molecular
Chemistry and Physics
www.mcp-journal.de

Figure 8. Time–temperature superposition of dynamic moduli of sodium neutralized sulfonated PS with emphasis on overlap at a) high-frequency, and b) low-frequency domain: the slope of the ratio of shift factors versus $1000/T$ in the inset plot (right) is $E_a/1000$ reflecting the activation energy of transient bonds. Adapted with permission.[123] Copyright 2017, American Institute of Physics c) Morphology and master-curve of dynamic moduli of KOH neutralized telechelic COOH-terminated PBd chains after equilibration for 300 (closed symbols) versus 2.4×10^8 s (open symbols). Adapted with permission.[130] Copyright 2009, American Chemical Society

separated the distinct temperature dependency of supramolecular dynamics from that of chain dynamics by applying tTS at low- and high-frequency domains, respectively, as shown in **Figure 8**a,b.[86,103,118,123]

In detail, the shift factor obtained at the high-frequency domain reflects the temperature dependency of segmental dynamics, as transient bonds are frozen, whereas the shift factor obtained at the low-frequency region returns that of both segmental and supramolecular dynamics. Therefore, their difference reflects the temperature dependency of transient bonds, as shown in the inset plot of Figure 8b. Importantly, it is actually possible to construct master curves from all data, which are "apparent" or "pseudo" master curves in the sense that they are only valid for one specific temperature.[119] Different from proper master curves in thermorheologically simple systems, where only the x-axis scale depends on the reference temperature via the multiplicative shift factor, the breadth/width of apparent master curves is now a function of absolute temperature, as shift factors differ in the high- and low-frequency domains governed by segmental and sticky dynamics, respectively. The actually relevant temperature is the "shift transition temperature", at which one chooses to switch from mastering (overlapping) the high-frequency end (segmental dynamics) to overlapping the low-

frequency processes (sticky dynamics). Thus, ignoring the violation of tTS in a broad range of time and temperature may result in unreliable master curves and consequent false interpretations of dynamics. Nevertheless, in some cases the temperature dependency of supramolecular dynamics is not significantly different from that of polymer dynamics, tTS is reported to be valid.[18,106,108]

The formation of aggregates undermines the additional temperature dependency of the pairwise supramolecular associations, as it collects and isolates them in sticker-rich domains and leaves the mobile bulk chains with a lower sticker content. If the system is dominated by stable clusters, a defined activation energy of debonding governs flow and the tTS rule is again partially applicable.[26,27,97] This effect is quite aligned with the variation of T_g upon clustering. Normally, a unique T_g is reported for homogeneous supramolecular systems in the absence of clustering, which is an increasing factor of the sticker content.[110,124] This is associated with the structural rigidity of supramolecular associations that increase the average local monomeric friction. In contrast, binary associations are screened out of the bulk upon the formation of clusters,[8,125,126] which can result in the appearance of two T_g transitions, arising from the matrix and segregated phases. This observation is typical for ionomers with

**ADVANCED
SCIENCE NEWS**

www.advancedsciencenews.com

**Macro-
molecular**
Chemistry and Physics

www.mcp-journal.de

rather stiff ionic clusters and significant amounts of immobilized polymer segments around them,[123,125] and is otherwise limited to strongly associating groups connected by rather short chains.[122,127,128] In all these systems, the modulus and terminal flow are strongly impacted by these clusters providing hydrodynamic reinforcement.[122,127,128] In contrast, many of the systems discussed above do not exhibit a second T_g.[103,118–122] This can be attributed to the overall small fraction of sticky groups and significant mobility inside of the clusters, which enables bulk-like mobility even in the stretched chains that are part of the micellar corona.[103] In these cases, modified glassy dynamics is an issue, but it acts very locally and modifies the energetics and kinetics of pairwise bond or cluster formation in a well-defined way, as recently highlighted by Ghosh and Schweizer.[129] So, as long as one well-defined aggregation mode prevails (pairs or clusters in a small size range), the sticky bond dynamics and thermodynamics can be well separable. Only in the case of unstable clusters, which undergo disintegration along with the terminal flow regime, a severe thermorheological complexity, or violation of tTS, is expected.[27,76,85] It is simply hopeless to construct apparent master curves for a system governed by more than two distinct activated processes. However, by increasing cluster stability, the measurable frequency region reflects more of the polymeric dynamics, and therefore, tTS validity is restored in this frequency range.

4.4. Interplay of Kinetics and Thermodynamics of Aggregation

Studies on the effect of molar mass on the aggregation tendency and chain dynamics in associative polymers are rather contradicting. It is no wonder, as the effect of molar mass is entangled with the compromise between kinetics and thermodynamics of aggregation. On the one hand, the phase separation tendency increases with molar mass, following the Flory–Huggins solution theory.[8,94] On the other hand, the slow dynamics of entangled chains, specifically in the presence of transient associations and aggregates require very long annealing times to form the expected equilibrium structure. Therefore, the results obtained for well-entangled systems could be always questionable, unless the formation of the equilibrium structure is confirmed before dynamic measurements.[130] In this regard, Stadler and coworkers have reported more than two orders of magnitude increase in the terminal relaxation of potassium hydroxide neutralized telechelic carboxylic acid-functionalized PBd chains that form percolated networks upon aggregation, by the prolongation of the thermal equilibrium step from 300 to 2.4×10^8 s, before rheological measurements, as shown in Figure 8c.[130]

But even for systems exhibiting sufficiently fast terminal dynamics and thus an equilibrium structure, systematic insights into the relation between the thermodynamics of aggregate formation and the sticky bond and sticky chain dynamics are limited. Most works follow a suggestion advocated by Rubinstein and Colby,[44,49] relating the bare (non-renormalized) sticky bond lifetime to the segmental timescale acting as attempt time:

$$\tau_b(T) = \tau_a(T) \exp\left\{ E_a^{st}/RT \right\} \tag{16}$$

Segmental dynamics thus provides the external clock and the "thermal bath" for overcoming the sticker activation energy E_a^{st}.

This quantity has been suggested to depend on the association enthalpy ΔH_{st}, which in turn is closely related to the sticker association equilibrium constant, and on an additional barrier for debonding: $E_a^{st} = \Delta H_{st} + \in_b$.[44] As analyzed recently,[131] current literature is rather inconsistent with regard to the presence (and attempted quantification) or the complete neglect of such a barrier. Many if not most works cited in this review follow the above starting point in their analyses (with or without an additional barrier $\in_b$), and compare $\tau_b(T)$, often claimed to be measurable directly by BDS, with rheological timescales to obtain information on bond lifetime renormalization. Notably, the recent model of Ghosh and Schweizer even invalidates the above equation and thus all such attempts on a fundamental level.[129] Therefore, the question about the interplay between the thermodynamics of aggregate formation and the relevant association lifetime should be considered an open challenge. Clearly, integrating these ideas into chain-level theories using, e.g., the tube model, which requires input in terms of effective friction coefficients arising from the aggregation dynamics, will be another important task for the future.

5. Conclusions

The nature-inspired aggregation of pairwise associations embedded in polymeric backbones with different lengths and topologies has been frequently utilized to form collective assemblies, whose structure ranges from well-defined ordered multi-dimensional structures to ill-defined non-ordered phase-separated nanodomains. The utility of such collective assemblies spans from supplementing material properties to aggregation-induced function or even aggregation-controlled structure that defines the material and its functions. The key factor for controlling the extent of aggregation-induced changes is the stability or dynamics of aggregates which mainly defines the structure and dynamics of the whole system. The theoretical background, modeling approaches, and experimental records on the dynamics of associative polymers in the presence of aggregates, as well as the specific considerations regarding the authenticity of the reported data are reviewed in this paper. We believe this overview not only encompasses exciting concepts to be utilized in designing aggregation-regulated materials but highlights existing gaps to be addressed by further fundamental studies.

Conflict of Interest

The authors declare no conflict of interest.

ADVANCED
SCIENCE NEWS

www.advancedsciencenews.com

Macro-
molecular
Chemistry and Physics

www.mcp-journal.de

[1] J.-M. Lehn, *Science* **2002**, *295*, 2400.

[2] J.-M. Lehn, *Interdisc. Sci. Rev.* **1985**, *10*, 72.

[3] D. B. Amabilino, D. K. Smith, J. W. Steed, *Chem. Soc. Rev.* **2017**, *46*, 2404.

[4] J. M. Lehn, in Makromolekulare Chemie. Macromolecular Symposia, Wiley Online Library, **1993**, p. 69/1.

[5] L. Brunsveld, B. J. Folmer, E. W. Meijer, R. P. Sijbesma, *Chem. Rev.* **2001**, *101*, 4071.

[6] M. Ahmadi, A. Jangizehi, E. van Ruymbeke, S. Seiffert, *Macromolecules* **2019**, *52*, 5255.

[7] S. Tang, B. D. Olsen, *Macromolecules* **2016**, *49*, 9163.

[8] A. Jangizehi, M. Ahmadi, S. Seiffert, *Mater. Adv.* **2021**, *2*, 1425.

[9] J. D. Fox, S. J. Rowan, *Macromolecules* **2009**, *42*, 6823.

[10] P. Yakovchuk, E. Protozanova, M. D. Frank-Kamenetskii, *Nucleic Acids Res.* **2006**, *34*, 564.

[11] S. Sivakova, S. J. Rowan, *Chem. Soc. Rev.* **2005**, *34*, 9.

[12] J. Poater, M. Swart, F. M. Bickelhaupt, C. F. Guerra, *Org. Biomol. Chem.* **2014**, *12*, 4691.

[13] T. P. Knowles, M. Vendruscolo, C. M. Dobson, *Nat. Rev. Mol. Cell Biol.* **2014**, *15*, 384.

[14] E. Gazit, *FASEB J.* **2002**, *16*, 77.

[15] E. Krieg, M. M. Bastings, P. Besenius, B. Rybtchinski, *Chem. Rev.* **2016**, *116*, 2414.

[16] I. M. Rasid, C. Do, N. Holten-Andersen, B. D. Olsen, *Soft Matter* **2021**, *17*, 8960.

[17] A. Jangizehi, M. Ahmadi, S. Pschierer, P. Nicolella, H. Li, K. Amann-Winkel, S. Seiffert, *Soft Matter* **2022**, *18*, 6836.

[18] M. Ahmadi, M. Ghanavati, *Polymer* **2020**, *211*, 123117.

[19] Y. Yang, M. W. Urban, *Chem. Soc. Rev.* **2013**, *42*, 7446.

[20] Y. Chen, A. M. Kushner, G. A. Williams, Z. Guan, *Nat. Chem.* **2012**, *4*, 467.

[21] J. Hentschel, A. M. Kushner, J. Ziller, Z. Guan, *Angew. Chem., Int. Ed.* **2012**, *51*, 10561.

[22] D. Mozhdehi, S. Ayala, O. R. Cromwell, Z. Guan, *J. Am. Chem. Soc.* **2014**, *136*, 16128.

[23] H. Goldansaz, A. Jangizehi, G. Nikravan, O. Verkinderen, B. Goderis, S. R. Ghaffarian, E. van Ruymbeke, M. Ahmadi, *React. Funct. Polym.* **2019**, *137*, 27.

[24] S. Sivakova, D. A. Bohnsack, M. E. Mackay, P. Suwanmala, S. J. Rowan, *J. Am. Chem. Soc.* **2005**, *127*, 18202.

[25] F. Herbst, S. Seiffert, W. H. Binder, *Polym. Chem.* **2012**, *3*, 3084.

[26] F. Herbst, K. Schröter, I. Gunkel, S. Gröger, T. Thurn-Albrecht, J. Balbach, W. H. Binder, *Macromolecules* **2010**, *43*, 10006.

[27] T. Yan, K. Schröter, F. Herbst, W. H. Binder, T. Thurn-Albrecht, *Macromolecules* **2014**, *47*, 2122.

[28] T. Yan, K. Schröter, F. Herbst, W. H. Binder, T. Thurn-Albrecht, *Macromolecules* **2017**, *50*, 2973.

[29] T. Aida, E. Meijer, S. I. Stupp, *Science* **2012**, *335*, 813.

[30] A. P. Schenning, E. Meijer, *Chem. Commun.* **2005**, 3245.

[31] P. Jonkheijm, A. Miura, M. Zdanowska, F. J. Hoeben, S. De Feyter, A. P. Schenning, F. C. De Schryver, E. Meijer, *Angew. Chem., Int. Ed.* **2004**, *43*, 74.

[32] F. J. Hoeben, L. M. Herz, C. Daniel, P. Jonkheijm, A. P. Schenning, C. Silva, S. C. Meskers, D. Beljonne, R. T. Phillips, R. H. Friend, *Angew. Chem.* **2004**, *116*, 2010.

[33] A. Ajayaghosh, S. J. George, *J. Am. Chem. Soc.* **2001**, *123*, 5148.

[34] A. Ajayaghosh, S. J. George, V. K. Praveen, *Angew. Chem.* **2003**, *115*, 346.

[35] P. Y. Dankers, T. M. Hermans, T. W. Baughman, Y. Kamikawa, R. E. Kieltyka, M. M. Bastings, H. M. Janssen, N. A. Sommerdijk, A. Larsen, M. J. Van Luyn, *Adv. Mater.* **2012**, *24*, 2703.

[36] E. A. Mol, Z. Lei, M. T. Roefs, M. H. Bakker, M. J. Goumans, P. A. Doevendans, P. Y. Dankers, P. Vader, J. P. Sluijter, *Adv. Healthcare Mater.* **2019**, *8*, 1900847.

[37] M. M. Bastings, S. Koudstaal, R. E. Kieltyka, Y. Nakano, A. Pape, D. A. Feyen, F. J. Van Slochteren, P. A. Doevendans, J. P. Sluijter, E. Meijer, *Adv. Healthcare Mater.* **2014**, *3*, 70.

[38] M. H. Bakker, C. C. Tseng, H. M. Keizer, P. R. Seevinck, H. M. Janssen, F. J. Van Slochteren, S. A. Chamuleau, P. Y. Dankers, *Adv. Healthcare Mater.* **2018**, *7*, 1701139.

[39] T. McLeish, *Adv. Phys.* **2002**, *51*, 1379.

[40] E. Van Ruymbeke, R. Keunings, C. Bailly, *J. Non-Newtonian Fluid Mech.* **2005**, *128*, 7.

[41] E. Van Ruymbeke, C.-Y. Liu, C. Bailly, *Rheol. Rev.* **2007**, *39*, 53.

[42] S. Milner, T. McLeish, R. Young, A. Hakiki, J. Johnson, *Macromolecules* **1998**, *31*, 9345.

[43] L. Leibler, M. Rubinstein, R. H. Colby, *Macromolecules* **1991**, *24*, 4701.

[44] M. Rubinstein, A. N. Semenov, *Macromolecules* **1998**, *31*, 1386.

[45] A. N. Semenov, M. Rubinstein, *Macromolecules* **1998**, *31*, 1373.

[46] M. Rubinstein, A. N. Semenov, *Macromolecules* **2001**, *34*, 1058.

[47] M. Cates, *Macromolecules* **1987**, *20*, 2289.

[48] Q. Chen, C. Huang, R. Weiss, R. H. Colby, *Macromolecules* **2015**, *48*, 1221.

[49] Q. Chen, G. J. Tudryn, R. H. Colby, *J. Rheol.* **2013**, *57*, 1441.

[50] X. Cao, X. Yu, J. Qin, Q. Chen, *Macromolecules* **2019**, *52*, 8771.

[51] D. Amin, A. E. Likhtman, Z. Wang, *Macromolecules* **2016**, *49*, 7510.

[52] Q. Chen, Z. Zhang, R. H. Colby, *J. Rheol.* **2016**, *60*, 1031.

[53] Z. Zhang, Q. Chen, R. H. Colby, *Soft Matter* **2018**, *14*, 2961.

[54] S. Wu, Q. Chen, *Macromolecules* **2021**, *55*, 697.

[55] M. Ahmadi, P. Nicolella, S. Seiffert, *Macromolecules* **2022**, *55*, 9960.

[56] E. B. Stukalin, L.-H. Cai, N. A. Kumar, L. Leibler, M. Rubinstein, *Macromolecules* **2013**, *46*, 7525.

[57] A. Semenov, J.-F. Joanny, A. Khokhlov, *Macromolecules* **1995**, *28*, 1066.

[58] A. Semenov, M. Rubinstein, *Macromolecules* **2002**, *35*, 4821.

[59] P.-G. De Gennes, *J. Chem. Phys.* **1971**, *55*, 572.

[60] M. Doi, S. F. Edwards, S. F. Edwards, *The theory of polymer dynamics*, Oxford University Press, Oxford **1988**.

[61] J. Des Cloizeaux, *Europhys Lett* **1988**, *5*, 437.

[62] E. Van Ruymbeke, C. Bailly, R. Keunings, D. Vlassopoulos, *Macromolecules* **2006**, *39*, 6248.

[63] R. Larson, *Macromolecules* **2001**, *34*, 4556.

[64] S. J. Park, S. Shanbhag, R. G. Larson, *Rheol. Acta* **2005**, *44*, 319.

[65] C. Das, N. J. Inkson, D. J. Read, M. A. Kelmanson, T. C. McLeish, *J. Rheol.* **2006**, *50*, 207.

[66] D. J. Read, D. Auhl, C. Das, J. Den Doelder, M. Kapnistos, I. Vittorias, T. C. McLeish, *Science* **2011**, *333*, 1871.

[67] M. Ahmadi, C. Bailly, R. Keunings, M. Nekoomanesh, H. Arabi, E. Van Ruymbeke, *Macromolecules* **2011**, *44*, 647.

[68] D. Daniels, T. McLeish, B. Crosby, R. Young, C. Fernyhough, *Macromolecules* **2001**, *34*, 7025.

[69] A. L. Frischknecht, S. T. Milner, A. Pryke, R. N. Young, R. Hawkins, T. C. McLeish, *Macromolecules* **2002**, *35*, 4801.

[70] T. McLeish, J. Allgaier, D. Bick, G. Bishko, P. Biswas, R. Blackwell, B. Blottiere, N. Clarke, B. Gibbs, D. Groves, *Macromolecules* **1999**, *32*, 6734.

[71] E. Van Ruymbeke, E. Muliawan, S. Hatzikiriakos, T. Watanabe, A. Hirao, D. Vlassopoulos, *J. Rheol.* **2010**, *54*, 643.

[72] Z. Wang, X. Chen, R. G. Larson, *J. Rheol.* **2010**, *54*, 223.

[73] M. Rubinstein, R. H. Colby, *Polymer Physics*, Oxford University Press, New York, **2003**.

[74] A. E. Likhtman, T. C. McLeish, *Macromolecules* **2002**, *35*, 6332.

[75] M. Doi, S. F. Edwards, *Thetheory of Polymer Dynamics*, Oxford University Press **1988**.

[76] M. Ahmadi, L. G. Hawke, H. Goldansaz, E. van Ruymbeke, *Macromolecules* **2015**, *48*, 7300.

[77] R. Jongschaap, R. Wientjes, M. H. Duits, J. Mellema, *Macromolecules* **2001**, *34*, 1031.

[78] E. Van Ruymbeke, Y. Masubuchi, H. Watanabe, *Macromolecules* **2012**, *45*, 2085.

[79] S. J. Park, R. G. Larson, *J. Rheol.* **2003**, *47*, 199.

[80] W. W. Graessley, *Synthesis and Degradation Rheology and Extrusion*, Springer, Berlin **1982**, 67.

[81] F. Zhuge, L. G. Hawke, C.-A. Fustin, J.-F. Gohy, E. Van Ruymbeke, *J. Rheol.* **2017**, *61*, 1245.

[82] W. Schmolke, M. Ahmadi, S. Seiffert, *Phys. Chem. Chem. Phys.* **2019**, *21*, 19623.

[83] H. Goldansaz, Q. Voleppe, S. Pioge, C.-A. Fustin, J.-F. Gohy, J. Brassinne, D. Auhl, E. Van Ruymbeke, *Soft Matter* **2015**, *11*, 762.

[84] E. Van Ruymbeke, J. Slot, M. Kapnistos, P. Steeman, *Soft Matter* **2013**, *9*, 6921.

[85] L. Hawke, M. Ahmadi, H. Goldansaz, E. Van Ruymbeke, *J. Rheol.* **2016**, *60*, 297.

[86] M. Ahmadi, A. Jangizehi, S. Seiffert, *Macromolecules* **2022**, *55*, 5514.

[87] C. W. Macosko, D. R. Miller, *Macromolecules* **1976**, *9*, 199.

[88] S. I. Hendrikse, S. P. Wijnands, R. P. Lafleur, M. J. Pouderoijen, H. M. Janssen, P. Y. Dankers, E. Meijer, *Chem. Commun.* **2017**, *53*, 2279.

[89] W. P. Appel, G. Portale, E. Wisse, P. Y. Dankers, E. Meijer, *Macromolecules* **2011**, *44*, 6776.

[90] P. Y. Dankers, M. J. van Luyn, A. Huizinga-van der Vlag, G. M. van Gemert, A. H. Petersen, E. W. Meijer, H. M. Janssen, A. W. Bosman, E. R. Popa, *Biomaterials* **2012**, *33*, 5144.

[91] R. E. Kieltyka, A. Pape, L. Albertazzi, Y. Nakano, M. M. Bastings, I. K. Voets, P. Y. Dankers, E. Meijer, *J. Am. Chem. Soc.* **2013**, *135*, 11159.

[92] M. Guo, L. M. Pitet, H. M. Wyss, M. Vos, P. Y. Dankers, E. Meijer, *J. Am. Chem. Soc.* **2014**, *136*, 6969.

[93] H. Feng, X. Lu, W. Wang, N.-G. Kang, J. W. Mays, *Polymers* **2017**, *9*, 494.

[94] M. Kossuth, D. Morse, F. Bates, *J. Rheol.* **1999**, *43*, 167.

[95] S. Ghiassinejad, K. Mortensen, M. Rostamitabar, J. Malineni, C.-A. Fustin, E. Van Ruymbeke, *Macromolecules* **2021**, *54*, 6400.

[96] A. Pape, M. Bastings, R. E. Kieltyka, H. M. Wyss, I. K. Voets, E. Meijer, P. Y. Dankers, *Int. J. Mol. Sci.* **2014**, *15*, 1096.

[97] X. Callies, C. Véchambre, C. Fonteneau, S. Pensec, J. M. Chenal, L. Chazeau, L. Bouteiller, G. Ducouret, C. Creton, *Macromolecules* **2015**, *48*, 7320.

[98] C. Véchambre, X. Callies, C. C. Fonteneau, G. Ducouret, S. Pensec, L. Bouteiller, C. Creton, J.-M. Chenal, L. Chazeau, *Macromolecules* **2015**, *48*, 8232.

[99] H. Kautz, D. Van Beek, R. P. Sijbesma, E. Meijer, *Macromolecules* **2006**, *39*, 4265.

[100] D. Van Beek, A. Spiering, G. W. Peters, K. Te Nijenhuis, R. P. Sijbesma, *Macromolecules* **2007**, *40*, 8464.

[101] M. Burnworth, L. Tang, J. R. Kumpfer, A. J. Duncan, F. L. Beyer, G. L. Fiore, S. J. Rowan, C. Weder, *Nature* **2011**, *472*, 334.

[102] J. Cortese, C. Soulié-Ziakovic, S. Tencé-Girault, L. Leibler, *J. Am. Chem. Soc.* **2012**, *134*, 3671.

[103] A. Mordvinkin, D. Döhler, W. H. Binder, R. H. Colby, K. Saalwächter, *Macromolecules* **2021**, *54*, 5065.

[104] R. Stadler, L. de Lucca Freitas, *Colloid Polym Sci* **1986**, *264*, 773.

[105] R. Stadler, L. de Lucca Freitas, *Polym. Bull.* **1986**, *15*, 173.

[106] L. L. De Lucca Freitas, R. Stadler, *Macromolecules* **1987**, *20*, 2478.

[107] L. De Lucca Freitas, R. Stadler, *Colloid Polym Sci* **1988**, *266*, 1095.

[108] L. De Lucca Freltas, J. Burgert, R. Stadler, *Polym. Bull.* **1987**, *17*, 431.

[109] M. Müller, E. Fischer, F. Kremer, U. Seidel, R. Stadler, *Colloid Polym Sci* **1995**, *273*, 38.

[110] A. Shabbir, H. Goldansaz, O. Hassager, E. van Ruymbeke, N. J. Alvarez, *Macromolecules* **2015**, *48*, 5988.

[111] H. Goldansaz, C. A. Fustin, M. Wubbenhorst, E. van Ruymbeke, *Macromolecules* **2016**, *49*, 1890.

[112] A. Jangizehi, S. R. Ghaffarian, W. Schmolke, S. Seiffert, *Macromolecules* **2018**, *51*, 2859.

[113] A. Jangizehi, S. R. Ghaffarian, W. Schmolke, S. Seiffert, *Macromolecules* **2020**, *53*, 491.

[114] A. Jangizehi, S. R. Ghaffarian, M. Ahmadi, *Polym. Adv. Technol.* **2018**, *29*, 726.

[115] A. Jangizehi, M. Ahmadi, S. Seiffert, *J. Polym. Sci., Part B: Polym. Phys.* **2019**, *57*, 1209.

[116] S. Seiffert, *Macromol. Rapid Commun.* **2016**, *37*, 257.

[117] G. Cui, V. A. Boudara, Q. Huang, G. P. Baeza, A. J. Wilson, O. Hassager, D. J. Read, J. Mattsson, *J. Rheol.* **2018**, *62*, 1155.

[118] A. Mordvinkin, M. Suckow, F. Böhme, R. H. Colby, C. Creton, K. Saalwächter, *Macromolecules* **2019**, *52*, 4169.

[119] A. Mordvinkin, D. Döhler, W. H. Binder, R. H. Colby, K. Saalwächter, *Phys Rev* **2020**, *125*, 127801.

[120] S. Ge, M. Tress, K. Xing, P.-F. Cao, T. Saito, A. P. Sokolov, *Soft Matter* **2020**, *16*, 390.

[121] B. Gold, C. Hövelmann, N. Lühmann, N. Székely, W. Pyckhout-Hintzen, A. Wischnewski, D. Richter, *ACS Macro Lett.* **2017**, *6*, 73.

[122] M. Tress, K. Xing, S. Ge, P. Cao, T. Saito, A. Sokolov, *Eur Phys J Spec Top* **2019**, *42*, 133.

[123] Z. Zhang, C. Huang, R. Weiss, Q. Chen, *J. Rheol.* **2017**, *61*, 1199.

[124] K. E. Feldman, M. J. Kade, E. Meijer, C. J. Hawker, E. J. Kramer, *Macromolecules* **2009**, *42*, 9072.

[125] A. Eisenberg, *Macromolecules* **1970**, *3*, 147.

[126] G. R. Goward, M. F. Schuster, D. Sebastiani, I. Schnell, H. W. Spiess, *J. Phys. Chem. B* **2002**, *106*, 9322.

[127] S. Ge, S. Samanta, M. Tress, B. Li, K. Xing, P. Dieudonné-George, A.-C. Genix, P.-F. Cao, M. Dadmun, A. P. Sokolov, *Macromolecules* **2021**, *54*, 4246.

[128] K. Xing, M. Tress, P. Cao, S. Cheng, T. Saito, V. N. Novikov, A. P. Sokolov, *Soft Matter* **2018**, *14*, 1235.

[129] A. Ghosh, K. S. Schweizer, *ACS Macro Lett.* **2021**, *10*, 122.

[130] F. J. Stadler, W. Pyckhout-Hintzen, J.-M. Schumers, C.-A. Fustin, J.-F. Gohy, C. Bailly, *Macromolecules* **2009**, *42*, 6181.

[131] K. Saalwächter, *Dynamics of Composite Materials*, Springer, Cham **2022**, 163.

Mostafa Ahmadi is a research associate at Johannes Gutenberg University Mainz since 2018. He obtained his Ph.D. from the Iran Polymer and Petrochemical Institute (2011), was a postdoc at Université catholique de Louvain (2011–2012), and an assistant professor at Amirkabir University of Technology (2012–2018). He was a Georg Forster fellow of the Alexander von Humboldt Foundation (2018–2021) and received an independent research grant from DFG (since 2021) to study the role of coordination geometry in metallo-supramolecular polymer networks.

Amir Jangizehi is a postdoct in the group of Prof. Sebastian Seiffert at Johannes Gutenberg University Mainz. After obtaining his Ph.D. in polymer science from Amirkabir University of Technology (Iran) in 2018, he spent one year as a postdoc at Karlsruhe Institute of Technology working on microfluidic templating of charged microscopic hydrogels. His research is focused on the physical chemistry of supramolecular polymers and hydrogels, with a particular view to nanostructural complexity and connectivity defects.

Kay Saalwächter completed his diploma in chemistry in 1997 at the Institute of Macromolecular Chemistry (University of Freiburg, Germany) and his doctorate in 2000 at the University of Mainz, working with H.W. Spiess at the MPI for Polymer Research. His Habilitation followed in 2004 back at the University of Freiburg. Since 2005 he has held a professorship of experimental physics at the Martin-Luther-University Halle-Wittenberg (Halle, Germany). Research in his group circles around the use and development of solid-state and solution NMR techniques to study structure and dynamics in polymeric, liquid-crystalline, biological, and other "soft" materials, applying also complementary techniques such as rheology, X-ray scattering and dielectric spectroscopy.

Sebastian Seiffert is professor for physical chemistry of polymers at Johannes Gutenberg University Mainz since 2016. He obtained his Ph.D. from Clausthal University of Technology (2007), was a postdoc at Harvard (2009–2010), and headed a junior research group at Helmholtz-Zentrum Berlin (2011–2014). His first faculty appointment was as associate professor for supramolecular polymer materials at Freie Universität Berlin (2014–2016). Sebastian's work was honored with the Reimund Stadler Award of the German Chemical Society (GDCh), an annual award by the Association of German University Professors in Chemistry (ADUC), and a young investigator award by the Polymer Networks Group (PNG).